




# fiducial reference measurements for satellite ocean colour

## D-130: Technical Report TR-5 “Protocols and Procedures to Verify the Performance of Fiducial Reference Measurement (FRM) Field Ocean Colour Radiometers (OCR) used for Satellite Validation

<b>Title</b>	Technical Report TR-5 “Protocols and Procedures to Verify the Performance of Fiducial Reference Measurement (FRM) Field Ocean Colour Radiometers (OCR) used for Satellite Validation
<b>Document reference</b>	FRM4SOC-TR5
<b>Project</b>	ESA – FRM4SOC
<b>Contract</b>	ESRIN/Contract No. 4000117454/16/1-SBo
<b>Deliverable</b>	D-130 (Technical Report TR-5)
<b>ATTN</b>	Craig Donlon ESA/ESTEC Technical Officer Keplerlaan 1 2201 AZ Noordwijk The Netherlands
<b>Version</b>	<b>1.2</b>
<b>Date issued</b>	10.02.2017

	<b>Prepared by</b>	<b>Signed By</b>	<b>Approved by</b>
Name:	Joel Kuusk	Riho Vendt	Craig Donlon
Organisation:	Tartu Observatory	Tartu Observatory	ESA/ESTEC
Position:	WP leader	Project manager	Technical Officer
Date:			
Signature:			

 <b>fiducial reference measurements for satellite ocean colour</b>	<b>ESRIN/Contract No. 4000117454/16/1-SBo</b> <b>Fiducial Reference Measurements for</b> <b>Satellite Ocean Colour (FRM4SOC)</b> <b>Technical Report TR-5</b>	Ref: FRM4SOC-TR5 Date: 10.02.2017 Ver: 1.2 Page 1 (60)
--	--	---


**Fiducial Reference Measurements for Satellite Ocean Colour (FRM4SOC)**  
– Laboratory Calibration Exercise 2 (LCE-2): Verification of Fiducial  
Reference Measurement Ocean Colour Radiometers (FRM OCR)

**D-130: Protocols and Procedures to Verify the Performance of Fiducial  
Reference Measurement (FRM) Field Ocean Colour Radiometers (OCR)  
used for Satellite Validation (TR-5)**

**TECHNICAL REPORT**

**Joel Kuusk, Ilmar Ansko, Viktor Vabson, Martin Ligi, Riho Vendt**



 <b>fiducial reference measurements for satellite ocean colour</b>	<b>ESRIN/Contract No. 4000117454/16/1-SBo</b> <b>Fiducial Reference Measurements for</b> <b>Satellite Ocean Colour (FRM4SOC)</b> <b>Technical Report TR-5</b>	Ref: FRM4SOC-TR5 Date: 10.02.2017 Ver: <b>1.2</b> Page 2 (60)
---	--	--

#### Document Control Table

<b>Title</b>	Technical Report TR-5 "Protocols and Procedures to Verify the Performance of Fiducial Reference Measurement (FRM) Field Ocean Colour Radiometers (OCR) used for Satellite Validation"
<b>Document reference</b>	FRM4SOC-TR5
<b>Project</b>	ESA – FRM4SOC
<b>Contract</b>	ESRIN/Contract No. 4000117454/16/1-SBo
<b>Deliverable</b>	D-130 Technical Report TR-5
<b>Version</b>	<b>1.2</b>
<b>Date Issued</b>	10.02.2017

#### Document Change Record

Index	Issue	Revision	Date	Brief description	Issued by
0.	1	0	31.08.2016	DRAFT	Riho Vendt
1.	1	1	07.12.2016	Updated schedule	Joel Kuusk
2.	1	2	10.02.2017	Major updates in many chapters	Joel Kuusk

#### Distribution List

Company/Organisation	Name	Format	No. of Copies
TO	Riho Vendt	Electronic file (PDF)	1
TO	Viktor Vabson	Electronic file (PDF)	1
TO	Joel Kuusk	Electronic file (PDF)	1
TO	Anu Reinart	Electronic file (PDF)	1
TO	Ilmar Ansko	Electronic file (PDF)	1
TO	Martin Ligi	Electronic file (PDF)	1
RBINS	Kevin Ruddick	Electronic file (PDF)	1
NPL	Andrew Banks	Electronic file (PDF)	1
PML	Gavin Tilstone	Electronic file (PDF)	1
ACRI-ST	Christophe Lerebourg	Electronic file (PDF)	1
LOV	David Antoine	Electronic file (PDF)	1
ESA ESTEC/EOP-SME	Craig Donlon	Electronic file – pdf and original (WORD) file	1 pdf 1 WORD file
ESA ESRIN/IPL-POE	Silke Bode	Electronic file – pdf and original (WORD) file	1 pdf 1 WORD file
ESA ESTEC	Marc Bouvet	Electronic file – pdf and original (WORD) file	1 pdf 1 WORD file





## Contents

Document Control Table .....	2
Document Change Record.....	2
Distribution List .....	2
Contents .....	3
Executive Summary.....	5
Acronyms and Abbreviations .....	6
List of symbols .....	7
1 Scope .....	8
2 Introduction .....	9
3 Organisation of the Comparison .....	10
3.1 Participation guidelines.....	10
3.2 Participants .....	10
3.3 Form of Comparison.....	10
3.4 Schedule .....	10
4 Facilities .....	11
4.1 Radiometric calibration.....	11
4.1.1 Calibration of irradiance sensors .....	11
4.1.2 Calibration of radiance sensors .....	13
4.2 Indoor intercomparison.....	13
4.2.1 Intercomparison of irradiance sensors .....	13
4.2.2 Intercomparison of radiance sensors.....	13
4.3 Outdoor intercomparison .....	14
4.3.1 Ancillary data and instruments.....	17
5 Traceability.....	19
5.1 Reference irradiance and radiance sources and relation to LCE-1.....	19
6 Measurement models .....	22
6.1 Radiometric sensitivity .....	22
6.1.1 Spectral Irradiance Calibrations .....	22
6.1.2 Spectral Radiance Calibrations.....	22
6.2 Tests before radiometric calibrations .....	24
6.2.1 Radiance sensor's FOV and response of cosine collectors.....	24
6.2.2 Polarization sensitivity .....	24
6.2.3 Non-linearity effects .....	24
6.2.4 Spectral stray light.....	25
6.2.5 Ambient temperature .....	25
6.3 Uncertainty contributions for laboratory calibrations and tests .....	26
6.3.1 Calibration certificate of the standard lamp.....	26
6.3.2 Lamp ageing.....	27
6.3.3 Interpolation .....	27
6.3.4 Lamp current and shunt.....	27
6.3.5 Diffuse reflectance plaque (certificate, correction if needed) .....	28





6.3.6	Distance.....	28
6.3.7	Reproducibility of adjustment (lamp, plaque, sensor) .....	28
6.3.8	Random effects (repeatability of spectra, and dark signal) .....	29
6.3.9	Environmental effects (temperature) .....	29
6.3.10	Non-linearity effects .....	29
6.3.11	Combined standard uncertainty .....	29
6.4	Indoor measurements .....	32
6.5	Outdoor measurements .....	32
6.6	Uncertainty budgets for outdoor measurements .....	33
7	Measurement instructions .....	36
7.1	Indoor comparison .....	36
7.1.1	Irradiance sensors .....	36
7.1.2	Radiance sensors .....	37
7.2	Outdoor comparison.....	38
7.2.1	The primary outdoor comparison .....	38
7.2.2	The secondary outdoor comparison .....	39
8	Calculations and data processing.....	41
8.1	Instrument data processing.....	41
8.2	Intercomparison .....	41
8.3	Data processing example: TriOS RAMSES hyperspectral radiometers .....	41
8.4	Uncertainty evaluation .....	42
9	Reporting of results .....	43
9.1	Indoor comparison .....	43
9.2	Outdoor comparison.....	43
10	Recommendations .....	44
10.1	Introduction .....	44
10.2	Intercomparison .....	44
10.3	Reference radiometer .....	45
10.4	Field calibration unit .....	46
11	Conclusions .....	47
12	References .....	48
Appendix A	Sample device file of a TriOS RAMSES spectroradiometer .....	51
Appendix B	Factory proposed data processing method for TriOS RAMSES spectroradiometers .....	52
Appendix C	Indoor comparison.....	56
C.1	Using the cleanroom.....	56
C.2	Measurement instructions .....	56
C.2.1	Irradiance sensors: .....	56
C.2.2	Radiance sensors: .....	57
Appendix D	Primary outdoor comparison .....	58
Appendix E	Secondary outdoor comparison.....	59
Appendix F	Data dissemination .....	60



## Executive Summary

This document, the “D-130: Technical Report TR-5 “Protocols and Procedures to Verify the Performance of Fiducial Reference Measurement (FRM) Field Ocean Colour Radiometers (OCR) used for Satellite Validation” is written following the contract ESRIN/Contract No. 4000117454/16/I-SBo between ESA and Tartu Observatory and the requirements stated by the Statement of Work, reference FRM4SOC Statement of Work, issue ,1 revision 6, dated 8th December 2015 for the ESA Invitation to Tender (ITT) ESA/AO/1-8500/15/I-SBo Fiducial Reference Measurements for Satellite Ocean Colour (FRM4SOC).

The document addresses the requirements to

- Be a written as a definitive handbook for those wishing to perform future LCE of this nature.
- Critically review the exact methodology used by teams to practically verify the calibration of FRM OCR using external reference SI traceable calibration sources and/or other approaches.
- Establish and document protocols and best practice to practically verify the performance of FRM OCR using external reference SI traceable calibration sources and/or other approaches.
- Define how to establish, present and maintain uncertainty budgets (determined in agreement with defined National Standards Laboratory protocols) for FRM OCR.
- Any other aspect considered relevant to defining relevant procedures and protocols.
- Address any other aspect required to ensure that TR-5 is complete.

The document is also provides base guidelines for organising the Laboratory Comparison Exercise LCE- 2. The purpose of the LCE-2 is to review critically the methodologies used by teams to practically verify the calibration of FRM OCR using external reference SI traceable calibration sources, and document protocols and best practice for it. The LCE-2 also serves as a preparation stage for the FICE-AAOT field intercomparison exercise. The LCE 2 can be divided into three sub-tasks:

- 1) Provide SI-traceable radiometric calibration for participating radiometers.
- 2) Organize indoor intercomparison in controlled environment.
- 3) Organize outdoor intercomparison over terrestrial water surface.

For that purpose, the method of direct comparison to an external reference will be used during the indoor intercomparison. A direct comparison between calibrated OCR instruments with a reference value combined from the measured values will be used at the second stage of the comparison exercise during the outdoor intercomparison. The final analysis of intercomparison results will be carried out by TO.

The main activities of LCE-2 take place from 08.05.2017 to 13.05.2017 at Tõravere, Estonia. The event is organised by Tartu Observatory, a public research and development authority, administered by the Estonian Ministry of Education and Research operating under the Research and Development Act, other laws, and international contracts. More details of the Agenda are available in the Implementation Plan for LCE-2 (D-140: Implementation plan for LCE-2 (LCE-2-IP).

The results of the LCE-2 will be published in D-170: Technical Report “Results from the First FRM4SOC Field Ocean Colour Radiometer Verification Round Robin Campaign” (TR-6) and D-160 “Data package containing all data collected during LCE-2” (LCE-2-DATA).

## Acronyms and Abbreviations

Acronym	Abbreviation
<b>AAOT</b>	Aqua Alta Oceanographic Tower
<b>ADC</b>	Analog-to-digital converter
<b>AERONET</b>	Aerosol Robotic Network
<b>CDOM</b>	Colored dissolved organic matter
<b>EO</b>	Earth Observation
<b>ESA</b>	European Space Agency
<b>EUMETSAT</b>	European Organisation for the Exploitation of Meteorological Satellites
<b>FICE</b>	Field Inter-Comparison Experiment
<b>FOV</b>	Field of View
<b>FWHM</b>	Full Width at Half Maximum
<b>FRM4SOC</b>	Fiducial Reference Measurements for Satellite Ocean Colour
<b>IOP</b>	Inherent Optical Properties
<b>ISO</b>	International Organization for Standardization
<b>LCE</b>	Laboratory Comparison Experiment
<b>LSF</b>	Line Spread Function
<b>MSI</b>	MultiSpectral Instrument
<b>MVSM</b>	Multi-spectral Volume Scattering Meter
<b>MVT</b>	Meris Validation Team
<b>NPL</b>	National Physical Laboratory
<b>OC</b>	Ocean Colour
<b>OLCI</b>	Ocean and Land Colour Instrument
<b>PAR</b>	Photosynthetically active radiation
<b>QTH</b>	Quartz Tungsten Halogen
<b>SI</b>	Système International d'Unités
<b>SLM</b>	Stray Light Correction Matrix
<b>SSF</b>	Slit-Scattering Function
<b>TO</b>	Tartu Observatory
<b>TR</b>	Technical Report
<b>TSM</b>	Total Suspended Matter
<b>UTC</b>	Coordinated Universal Time
<b>VSF</b>	Volume Scattering Function



## List of symbols

Symbol	Definition
$E$	Irradiance
$E_d$	Downwelling irradiance
$G_C$	Gain amplification factor
$\lambda$	Wavelength
$L$	Radiance
$L_d$	Downwelling radiance
$L_u$	Upwelling radiance
$L_w$	Water-leaving radiance
$n$	Refractive index of water
$R_E$	Irradiance responsivity
$R_{RS}$	Remote sensing reflectance
$\tau_a$	Aerosol optical thickness
$\theta_s$	Solar zenith angle
$\theta_v$	View zenith angle
$w_s$	Wind speed





## 1 Scope

The core action of the FRM4SOC project is to ensure that ground-based measurements of ocean colour parameters are traceable to SI standards in support of ensuring high quality and accurate Sentinel-2 MSI and Sentinel-3 OLCI products. The FRM4SOC project contributes directly to the work of ESA and EUMETSAT to ensure Sentinel-3 OLCI and Sentinel-2 MSI instruments are validated in orbit.

LCE-2 links the OC field measurements to the SI-traceable calibration and verifies whether different instruments measuring the same object can provide consistent results within the uncertainty limits.

Involvement of all relevant expertise available in Europe and worldwide is in line with the objectives of the project and in the interest of the EO/ocean colour community. Therefore, it is anticipated that all interested parties in this wider community, but outside the Consortium, should be able to participate in the comparison exercise as external participants. Tartu Observatory (TO) will publish a global open invitation for LCE-2 to involve as many active users of Field Ocean Colour Radiometers as possible. Information about participating instruments will be gathered and TO will work together with the participants in order to make sure that all the necessary soft- and hardware for mounting and operating the instruments in the lab and during the outdoor intercomparison will be available for the time of LCE-2. The OC radiometers participating in the exercise will be gathered to TO prior LCE-2 for absolute radiometric calibration. Participants will join afterwards for comparison measurements. TO will help the participants with all aspects concerning travel, accommodation, customs, shipping of instruments, etc.

## 2 Introduction

The purpose of the LCE-2 is to review critically the methodologies used by teams to practically verify the calibration of FRM OCR using external reference SI traceable calibration sources, and document protocols and best practice for it.

The LCE-2 will serve as a preparation stage for the FICE-AAOT field intercomparison exercise. The LCE-2 can be divided into three sub-tasks:

- 1) Provide SI-traceable radiometric calibration for participating radiometers
- 2) Organize indoor intercomparison in controlled environment
- 3) Organize outdoor intercomparison over terrestrial water surface

It is not feasible to calibrate all parameters (wavelength accuracy, stray light, field of view, temperature stability, linearity, angular response for irradiance sensors, etc.) of all the participating instruments during LCE-2. However, all participants of LCE-2 are encouraged to have their instruments as well characterised as possible prior to LCE-2. Absolute radiometric calibration will be performed for all the participating radiometers just before the LCE-2.

LCE-2 will take place before FICE-AAOT on 08.05.2017 – 13.05.2017. It will serve as a training session for the participants of FICE-AAOT as well as provide SI-traceable radiometric calibration of participating radiometers. Previous inter-comparison of ocean colour radiometers has shown that the consistency of results improved when all the instruments participating in the inter-comparison were radiometrically calibrated in the same laboratory [1].

TO will serve as the main organizer for this comparison, supported by NPL. TO will be responsible for inviting participants and for the analysis of data, following appropriate processing by individual participants. TO will be the only organisation to have access and to view all data from all the participants. This data will remain confidential to the participant and TO at all times, until the publication of the report showing results of the comparison to participants.

### 3 Organisation of the Comparison

The event is organised by Tartu Observatory, a public research and development authority, administered by the Estonian Ministry of Education and Research operating under the Research and Development Act, other laws, and international contracts.

#### 3.1 Participation guidelines

By their declared intention to participate in this key comparison, the participants accept the general instructions and the technical protocols written down in this document and commit themselves to follow the procedures strictly.

Registration will be opened from 01.11.2016 to 20.12.2016. Registration will be made through online form on the project's website, which will follow the structure seen in appendices 1 and 2 of the LCE-2 implementation plan. During the registration, the participants have to fill in the description about the radiometers they are bringing to the event. As the site for field measurements is with limited size, only one set of radiometers is recommended per participating institute. The acceptance/rejection on the participation will be sent to all applicants in the beginning of January 2017.

#### 3.2 Participants

As the maximum number of participants to be handled is 15, then the participants for LCE-2 will be selected by the following criteria in the following order:

- 1) Partnership in FRM4SOC
- 2) Participation in FICE
- 3) Participation in LCE-1
- 4) Fully characterised radiometers of the participant
- 5) For the rest, first come, first served

#### 3.3 Form of Comparison

The comparison exercise will practically verify the calibration of FRM OCR provided by Tartu Observatory. For that purpose, the method of direct comparison to an external reference will be used during the indoor intercomparison. A direct comparison between calibrated OCR instruments with a reference value combined from the measured values will be used at the second stage of the comparison exercise during the outdoor intercomparison [2], [3], [4].

#### 3.4 Schedule

The following schedule is planned for LCE-2.

- 1) Registration opened: 01.11.2016 – 20.12.2016
- 2) Confirmed list of participants: beginning of January 2017
- 3) Arrival of the participating instruments to TO: 24.04.2017
- 4) Main activities of LCE-2: 08.05.2017 – 13.05.2017.

More details of the Agenda are available in the Implementation Plan for LCE-2 (LCE-2-IP).

## 4 Facilities

### 4.1 Radiometric calibration

The radiometric calibration and indoor intercomparison will take place at Tartu Observatory, located in Tõravere, Estonia. TO has modern, well equipped facilities for research work, an excellent visitor centre, and new laboratory complex. In 2012, a new laboratory complex at the premises of TO has been established for development and testing of new technologies including stations for development, prototyping, and assembly of electronics; facilities for climatic, thermal-vacuum, vibration, shock, and electromagnetic compatibility (EMC) testing; workshop for mechanical construction and repair works of scientific instruments. The laboratories have independent and automatic control of temperature and humidity. Special conditions as electrostatic discharge protected environment (ESD), anechoic chamber, and cleanrooms (EN ISO 14644 Class 8) have been established. Three rooms in cleanroom environment with total area of 100 m<sup>2</sup> are available for optical measurements. Optical laboratory includes passive damping setup tables, one of them on separately built foundation for vibration-free measurements.

The key elements of the existing laboratory equipment for establishment of the spectral irradiance scale include: FEL lamps, 1000 W with spectral irradiance calibrated in the wavelength range of (250...2500) nm and relative uncertainty 1.2%...8% depending on wavelength; filter radiometer based on three-element Si trap detector for the spectral range of (340...950) nm; filter radiometer based on three-element InGaAs trap detector for the spectral range of (900...1550) nm; diffuse reflectance targets with diameter of (10...30) cm, and calibrated reflectance factor of 2%...99%; 450 W stabilized Xe arc source (Newport/Oriel); radiometric power supplies for calibration lamps; scanning monochromators, including double LOMO SDL-1 with spectral range of (200...6000) nm, and Bentham DTMS300 with spectral range of (200...2500) nm, fully automated for spectral measurements; linear and rotary translation stages; stabilized He-Ne laser (633 nm, output power of 1.5 mW, long-term stability 0.2%, from Thorlabs); electrically calibrated pyroelectric radiometer RS-5900 in the spectral range of (250...3000) nm, input power 5 µW...100 mW, with relative uncertainty of 1%; integrating spheres with diameters from 5 cm to 1.2 m; calibrated power supplies and measurement electronics, photomultiplier detectors, environmental testing boxes, optical shutters, mounting tables, rubidium based high precision reference frequency source with the long term frequency stability of 10<sup>-12</sup>.

In order to assure and demonstrate the reliability of the calibration services, the quality management procedures are being developed and applied. For establishment of the metrological traceability of measurement results the reference instruments are calibrated at National Metrology Institutes or accredited calibration laboratories (NPL, UK; MRI-MIKES, Finland; Metrosert, Estonia). The stability of the reference standards and measurement instruments is regularly monitored in the intermediate period of subsequent calibrations.

Regular calibration and characterisation of several common types of radiometers used for OCR (e.g. TriOS RAMSES, Satlantic TACCS, Water Insight WISP-3) is performed at the laboratories of TO. A special study for characterisation of the OCR radiometers for quantification of the effect of stray light and the possible methods for its correction is in progress [5], [6].

#### 4.1.1 Calibration of irradiance sensors

Link to the international SI scale is provided via an FEL lamp calibrated at NPL (Figure 11). The lamp is powered by a stabilized radiometric power supply Newport/Oriel 69935 ensuring proper polarity as marked on the lamp. The lamp is operated in constant current mode. A custom designed circuit is used for monitoring the lamp current through a 10 mΩ shunt resistor P310 and providing feedback to the power supply. Lamp current is stabilized to better than ±1 mA. The same feedback unit is used for logging the lamp current and voltage. Voltage is measured with a 4-wire sensing method from the connector of the lamp socket. The power supply is turned on and slowly ramped-up to the working current of the lamp. Calibration measurements may be started after at least a 20 min warm-up time. During calibration the voltage across the lamp terminals is also measured, and compared to the voltage measured during the last calibration of the lamp. A significant change in the lamp's operating voltage indicates that it is no longer usable as a reliable working standard of spectral irradiance. On completion of the calibration, the lamp current is slowly ramped down to avoid thermally shocking the filament.

The lamp and OC radiometer being calibrated are mounted on an optical rail that passes through a bulkhead which separates the lamp and radiometer during calibration (Figure 1). A computer-controlled electronic shutter Melles Griot 04UTS268 with a Ø64 mm aperture is attached to the bulkhead. The shutter is used for dark signal measurements during calibration. Two additional baffles with Ø60 mm





apertures are placed between the bulkhead and the radiometer at 50 mm and 100 mm distances from the bulkhead. The OC radiometer being calibrated is mounted next to a filter radiometer on a computer-controlled linear translation stage which allows perpendicular movement with respect to the optical rail. The positions of both radiometers are carefully adjusted before calibration and the translation stage positions saved in the controlling software. This allows fast and accurate swapping of the radiometers when the lamp is turned on. The filter radiometer is used for monitoring possible long term drifts of the standard lamp. The filter radiometer is based on a 3-element trap detector with Hamamatsu S1337-11 windowless Si photodiodes and temperature-controlled bandpass filters with peak transmittances at nominal wavelengths 340 nm, 350 nm, 360 nm, 380 nm, 400 nm, 450 nm, 500 nm, 550 nm, 600 nm, 710 nm, 800 nm, 840 nm, 880 nm, 940 nm, and 980 nm. The photocurrent of the filter radiometer is amplified and digitized with a Bentham 487 current amplifier with integrating ADC. Newport 350B temperature controller is used for stabilizing the temperature of the bandpass filters. The filters are changed manually and it takes about two minutes for the temperature of the filter to stabilize. As the OC radiometer and filter radiometer cannot be used simultaneously, an additional monitor detector is used for recording short time changes in the lamp intensity during calibration. The distance between the lamp and the radiometer is measured with a custom designed measurement probe. One end of the probe is placed against the socket of the lamp and the other end of the probe has two lasers with beams intersecting at 120° angle (Figure 17). The point of intersection defines the other endpoint of the probe. Such a design allows contactless distance measurement and there is no need for touching the diffuser surface of the radiometer. The contactless probe is especially handy if the diffuser is covered with a protective glass dome. The measurement accuracy of the distance probe is better than 0.2 mm.

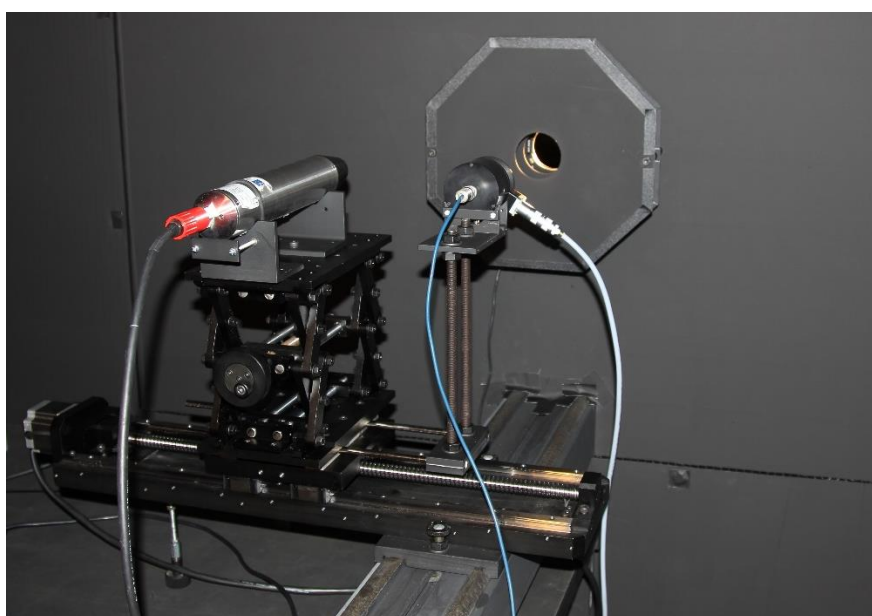
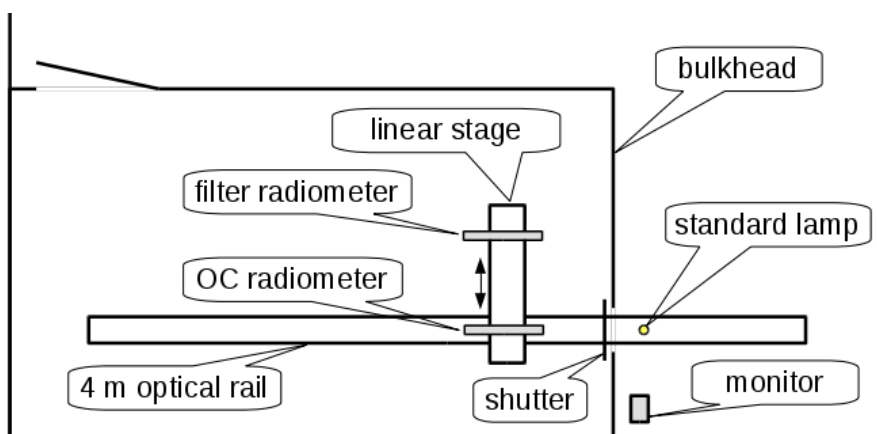


Figure 1: Irradiance sensor calibration setup of TO.



#### 4.1.2 Calibration of radiance sensors

Radiance sensor calibration setup (Figure 2) is based on the lamp/plaque method and utilizes the same components as the irradiance sensor calibration setup. A Sphere Optics sg3151 (200×200) mm calibrated white reflectance standard is mounted on the linear translation stage next to the filter radiometer. Normal incidence for the illumination and 45° from normal for viewing are used. The panel is calibrated in the same illumination and viewing conditions at NPL during LCE-1 (Figure 11). A mirror in a special holder and an alignment laser are used for aligning the plaque and radiance sensor.

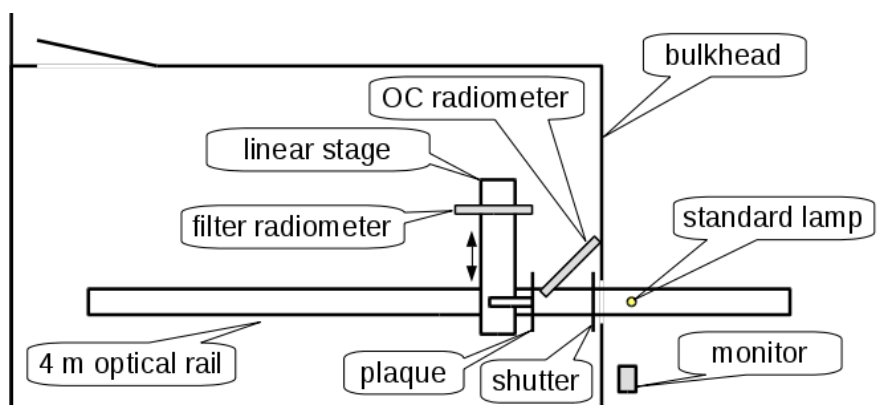


Figure 2: Radiance sensor calibration setup of TO.

#### 4.2 Indoor intercomparison

The indoor intercomparison will take place at Tartu Observatory, Estonia. Stable radiance and irradiance sources are used for verifying the performance of OC radiometers.

##### 4.2.1 Intercomparison of irradiance sensors

An FEL lamp (Figure 3) will be used as a stable irradiance source for indoor intercomparison. The power supply, feedback unit, monitor detector, and distance measurement probe will be the same as used for the radiometric calibration, but the FEL lamp will be different.



Figure 3: An FEL lamp will be used as a stable irradiance source for indoor intercomparison.

##### 4.2.2 Intercomparison of radiance sensors

A Bentham ULS-300 integrating sphere with internal illumination (Figure 4) is used as a stable radiance source. ULS-300 is a Ø300 mm integrating sphere with Ø100 mm target port. According to the manufacturer the uniformity of radiance over the output aperture is  $\pm 0.05\%$  independent of the intensity setting. The sphere has a single 250 W quartz tungsten halogen light source and an 8-branch fibre for transporting the light into the sphere. The intensity of light inside the sphere can be changed with a variable mechanical slit placed between the light source and the fibre bundle. This design allows changing the intensity while maintaining the spectral composition of light which corresponds to



correlated colour temperature ( $3100 \pm 20$ ) K. The lamp is powered by a Bentham 605 stabilized power supply. A Gigahertz-Optik VL-3701-1 broadband illuminance sensor attached directly to the sphere is used as monitor detector. The monitor current is recorded by a proprietary datalogger.

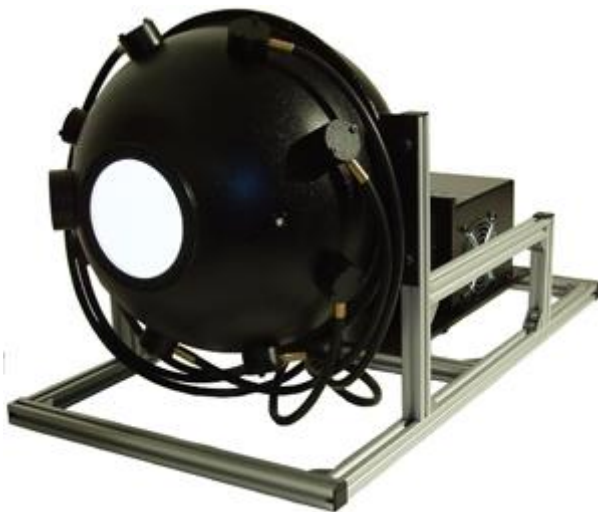


Figure 4: Bentham ULS-300 integrating sphere.

### 4.3 Outdoor intercomparison

The outdoor intercomparison will take place at Lake Kääriku, Estonia,  $58^{\circ} 0' 5''$  N,  $26^{\circ} 23' 55''$  E (Figure 5). Kääriku is a small village located in south eastern Estonia, 30 km south of Tõravere (approximately 45 minutes' drive by car).

Lake Kääriku is a eutrophic lake. It has an irregular shape with the surface area of 19.8 ha (length 650 m, width 550 m). It has rather small catchment area ( $4.8 \text{ km}^2$ ). Maximum depth is 5.9 m, with an average of 2.6 m. The water colour is greenish-yellow, measured transparency (Secchi disk depth) is 1.8 m. The average chlorophyll content  $\text{Chl} = 11.9 \text{ mg m}^{-3}$ , total suspended matter content is  $\text{TSM} = 3.5 \text{ g m}^{-3}$ , diffuse attenuation coefficient of downwelling irradiance  $K_d(\text{PAR}) = 1.3 \text{ m}^{-1}$ . The bottom is muddy. The lake has only a weak inflow, water exchanges twice a year. According to EU Water Framework Directive, it is unstratified lake with medium alkalinity (type II). It is classified as macrophyte-dominated shallow lake. Macrophytic vegetation is dominated by helophytes.

Lake Kääriku has a 50 m long pier and a diving platform on the southern coast (Figures 5 and 6). The diving platform has two levels. The upper level is 5.7 m above the water surface and the handrail of the upper level is 6.8 m above the water surface (

Figure 7). Depth of water around the diving platform is 2.6 m to 3.6 m (Figure 8). Depth was measured with a Plastimo Echotest 2 handheld depth sounder. Closest trees are about 65 m south of the platform, the treetops are less than  $20^{\circ}$  above the horizon when viewed from the upper level of the platform. The modelled shadows of the tower around noon and two hours before noon in the middle of May can be seen in Figure 9. The cones in Figure 9 represent the  $7^{\circ}$  field-of-view (FOV) of a TriOS RAMSES spectroradiometer in the typical view configuration of  $40^{\circ}$  nadir angle and  $135^{\circ}$  relative azimuth angle from the principal plane.



Figure 5: Lake Kääriku.



Figure 6: Pier and diving platform of Lake Kääriku.





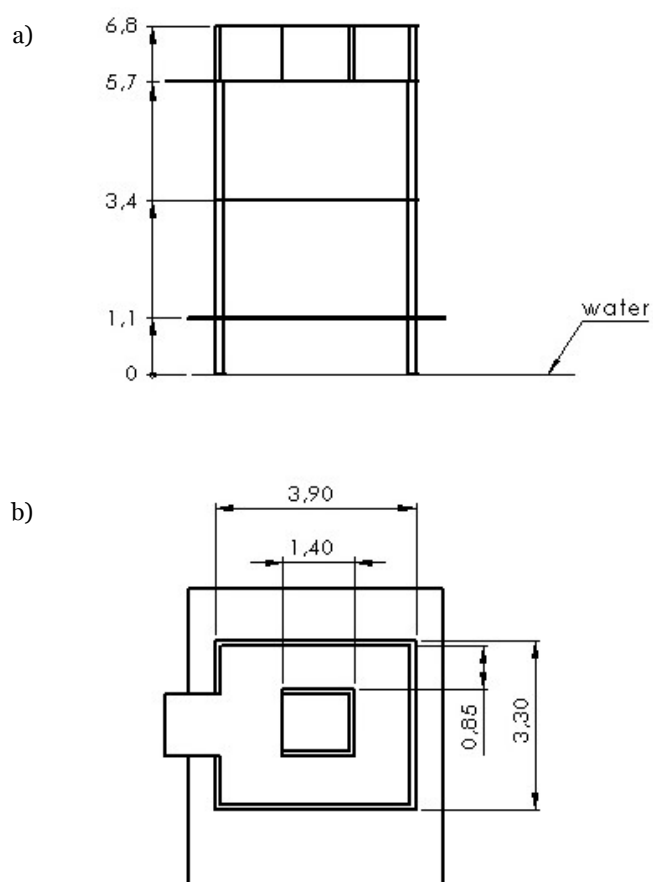


Figure 7: Dimensions of the diving platform in metres, a) – front view, b) – top view.

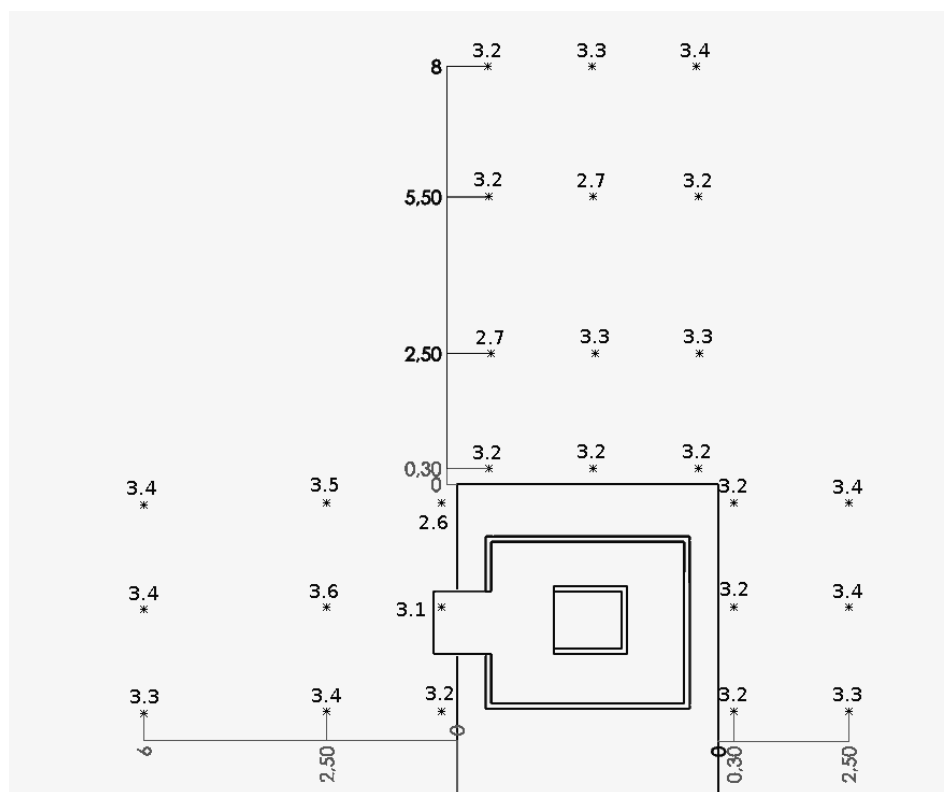


Figure 8: Depth of water around the diving platform of Lake Kääriku. Units are metres.



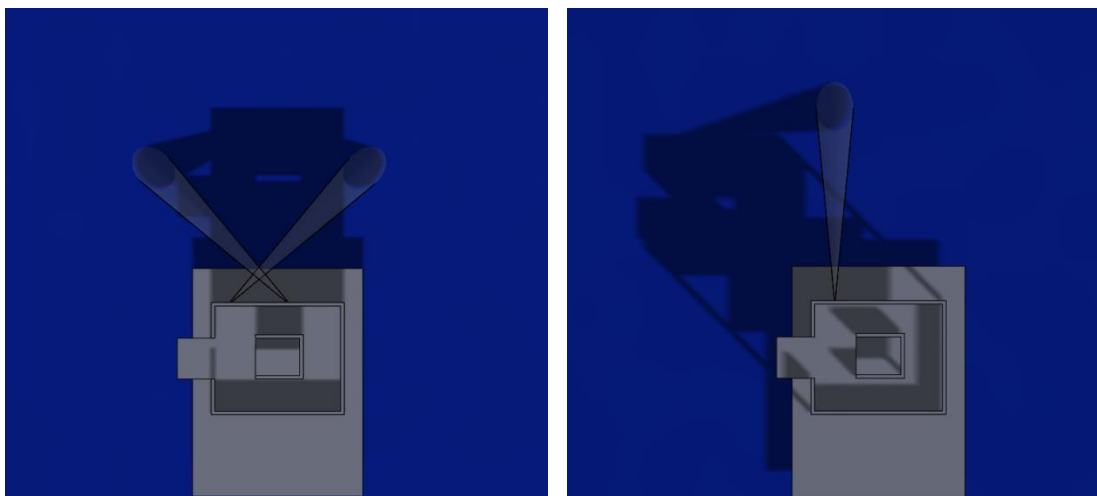


Figure 9: Modelled shadow of the tower around noon (left) and 2 hours before noon (right) in the middle of May. Cones represent the field-of-view of TriOS RAMSES spectroradiometer.

#### 4.3.1 Ancillary data and instruments

Chlorophyll-a concentration is measured in the laboratory of Limnological Station of the Estonian University of Life Sciences. Water is strained through Whatman GF/F glass microfiber filter with 0.7  $\mu\text{m}$  pore size. Chlorophyll is extracted from the filter with 96 % ethanol and the solution is analyzed spectrophotometrically according to ISO 10260:1992 standard. The concentration of chlorophyll-a is calculated according to the Lorenzen method [7].

The concentration of total suspended matter (TSM) is measured by straining the carefully mixed water sample through a glass microfiber filter and drying the filter in an oven. The mass of TSM is determined by weighing and concentration is calculated as the ratio of masses of TSM and water sample.

Absorption of coloured dissolved organic matter (CDOM) is measured in (280...800) nm spectral range with Hitachi U-3010 Dual Beam spectrophotometer after straining the sample through a filter with 0.45  $\mu\text{m}$  pore size. Distilled water is used as a reference.

Phytoplankton species composition and phytoplankton biomass is determined using inverted light microscope Ceti Versus, Belgium; magnifications 100 $\times$  and 400 $\times$  according to the technique proposed in [8]. At least 400 counting units are counted. The mean volume of each species is measured by approximating the shape of the species to the closest simple geometric form. In case of filamentous forms the length of at least 50 trichomes is measured and the mean length is then used for biomass (wet weight) calculation.

Phytoplankton pigment specific absorption is measured with Hitachi U-3010 Dual Beam spectrophotometer equipped with integrating sphere. Sample is filtrated through GF/F filter and the light transmission of both, pigmented and non-pigmented aquatic particles is measured according to method described in [9]. NaClO is used for bleaching. Chlorophyll-specific absorbance is calculated as difference between bleached and non-bleached filter:  $aph = atot - adp$ , and chlorophyll-a specific absorption coefficient is calculated as  $aph / (chl\ a + phaeopigment\ concentration)$ .

Transparency of water is evaluated with a Secchi disk. There are several variants of Secchi disks, TO uses a  $\varnothing 20$  cm white disk (Figure 10). Secchi disk is lowered into the water until it disappears from view. Attenuation coefficient of water can be estimated from the immersion depth [10].



Figure 10: Secchi disk.

Depth of water is measured with a Plastimo Echotest 2 handheld depth sounder or with a tape measure. Wind speed is measured with a handheld anemometer API-49. Air and water temperatures are measured with a custom-designed digital thermometer based on a Dallas Semiconductor DS18B20 temperature sensor.

Nikon D5100 digital camera with a Sigma 4.5 mm F2.8 EX DC circular fisheye lens is available for recording cloudiness. The camera can be programmed to time-lapse capture.

AERONET sun photometer Cimel CE318 is located in Tõravere, 30 km north of Lake Kääriku. Atmospheric ozone and water vapour content and aerosol optical depth can be measured on site with Cimel CE-318N-EM-S9 and Microtops II sun photometers.



## 5 Traceability

Metrological traceability means that an unbroken chain of calibrations is in place for each measurement result relating it with a suitable reference – a primary realization of a respective SI unit - whereby all calibrations of the chain are documented and contribute to the measurement uncertainty [11]. For establishment of the metrological traceability at TO the reference instruments are calibrated at National Metrology Institutes or accredited calibration laboratories (NPL, UK; MRI-MIKES, Finland; Metroser, Estonia, and TO, Estonia).

### 5.1 Reference irradiance and radiance sources and relation to LCE-1

The spectral irradiance scale of TO is realized with quartz tungsten halogen (QTH) incandescent lamps. The radiometric standard lamps are of FEL type: 1000 W, quartz-halogen, tungsten double-coiled filament, operated in the open air with coil in vertical position. The lamps are operated with constant direct current of 8.100 A or 8.200 A, depending on the type. The voltage across lamp terminals is approximately (105...110) V. Working time of the lamp after calibration is carefully recorded in order to account for uncertainty increase due to temporal instability of the lamps. Typical ageing rate during a simulated use cycle of a pre-selected, pre-aged modified FEL lamps is described in [12]–[14]. Each lamp has its own alignment jig. The alignment jig is placed in front of the lamp with the grooved surface directed towards the detector. Distance between the lamp and detector is normally 500 mm, and measured with respect to the reference plane defined as the front surface of the lamp socket. Other reference planes like the centre of filament or the surface of the alignment jig are not to be used.

For determination of spectral radiance, the radiation from a calibrated diffuse reflectance plaque is measured. The plaque is illuminated by a calibrated lamp of known spectral irradiance, placed at the distance of at least 500 mm from the plaque. The radiance input optics of the instrument being calibrated is placed at view angle  $45^\circ$  from normal in front of the plaque at a distance of several centimetres, allowing the FOV to be filled by reflected radiation.

The link to the SI in LCE-2 is provided by the three standard lamps calibrated at NPL during the LCE-1 (Figure 11, and Figure 12). The traceability of radiance measurements in LCE-2 is additionally provided by the reference radiometer calibrated at NPL during the LCE-1.

The radiometric standard (FEL) lamps of TO have been previously calibrated at the Metrology Research Institute, Aalto University, MIKES. The electrical instruments (multimeters, shunt resistors, and current-to-voltage converters) used for operating the lamp and recording the measurement signals are calibrated at national standard of electric quantities, Metroser Ltd (Figure 11). Diffuse reflectance plaque is calibrated in  $8^\circ$ /hemispherical illumination/view configuration at Labsphere Inc. and in  $0^\circ/45^\circ$  configuration during LCE-1 at NPL. Length and distance measurements are traceable to the national standard of length, and temperature measurements to national standard of temperature, Metroser Ltd. Some radiometric, electrical, length and temperature calibrations are done in-house at TO.

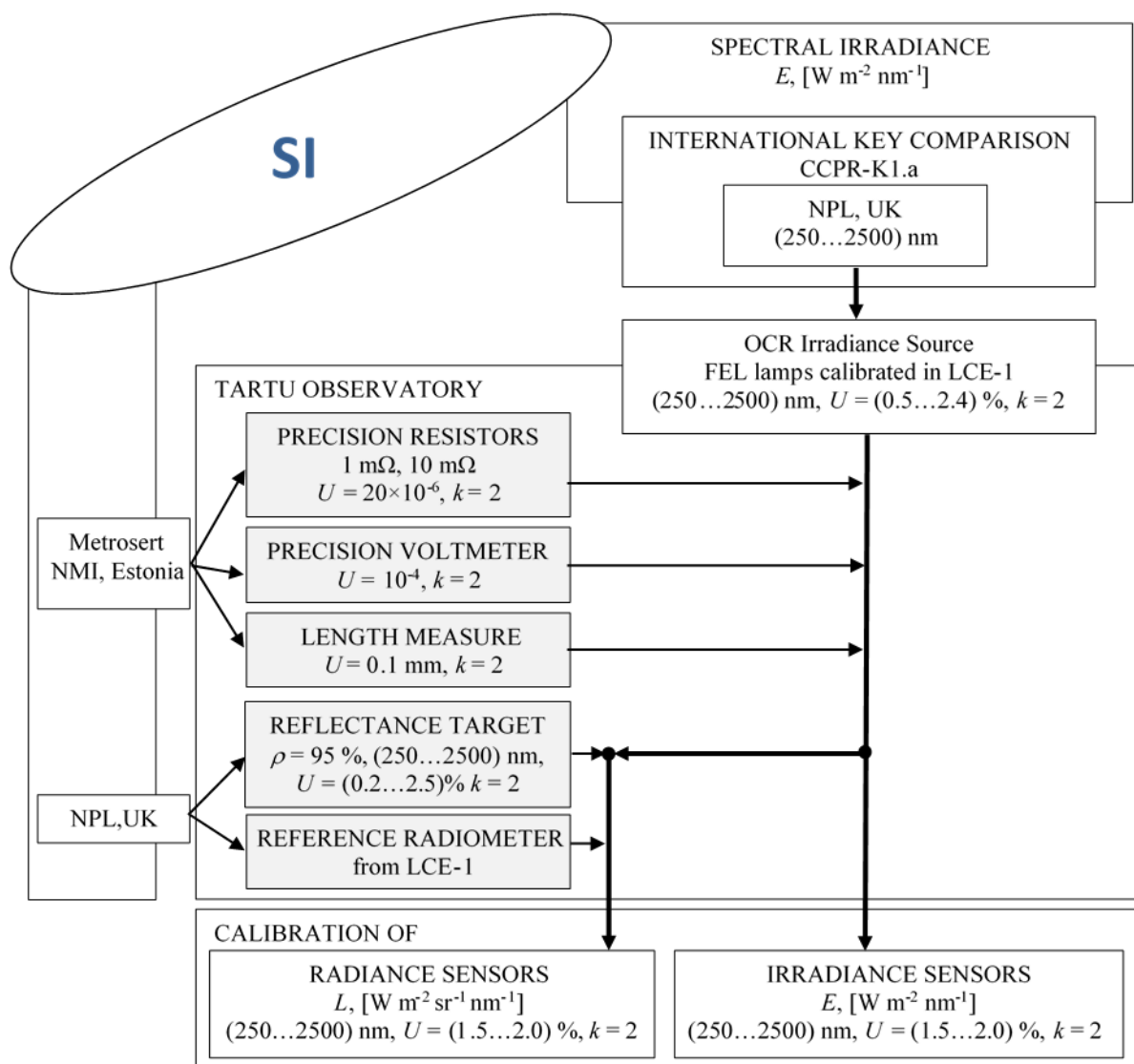


Figure 11: Metrological traceability to the units of SI in calibration of irradiance and radiance sensors in LCE-2.

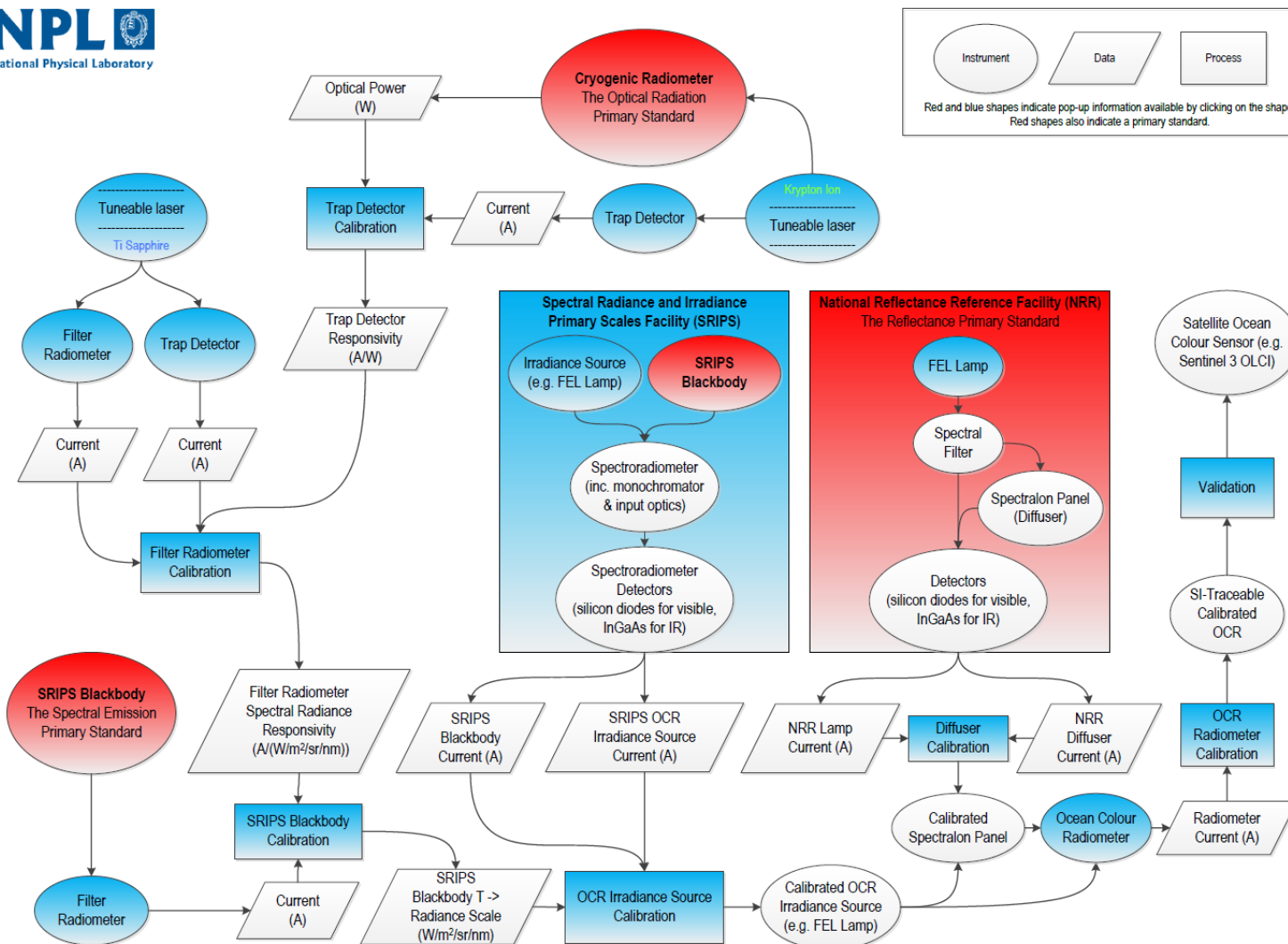


Figure 12: Overall metrological traceability to the units of SI in FRM4SOC.



## 6 Measurement models

Measurement model is usually a function, which describes the output quantity  $Y$  about which information is required as a function  $f$  of input quantities  $X_i$  which are measured or about which information is available:  $Y = f(X_1, X_2, X_3 \dots)$  [15]. Model function allows also solve the problem of uncertainty propagation from input quantities  $X_i$  through  $f$  to the output quantity  $Y$  if the uncertainties are negligibly small compared with the determined quantity values  $x_i$ . In the following paragraphs 6.1 to 6.5 basic models relevant for LCE-2 are described.

### 6.1 Radiometric sensitivity

#### 6.1.1 Spectral Irradiance Calibrations

For determination of spectral responsivity of the radiometer  $R_E(\lambda)$  for the irradiance [16]–[21], it is calibrated against a known source normally placed at fixed distance from the entrance optics of the radiometer. If an irradiance sensor at lamp distance of 500 mm is saturated, then in order to reduce the irradiance level the distance between the lamp and sensor should be increased. A new irradiance level  $E(\lambda, l)$  can be determined by measuring the optical signal with the aid of standard filter radiometer at the arbitrary filter wavelength as:

$$E(\lambda, l) = E(\lambda, l_0) \frac{F(l) - F_0(l)}{F(l_0) - F_0(l_0)}. \quad (1)$$

Here  $E(\lambda, l_0)$  [mW m<sup>-2</sup> nm<sup>-1</sup>] is the irradiance from the calibration certificate of the lamp at  $l_0=500$  mm,  $F(l)$  is the signal at  $l$  and  $F_0(l)$  is the respective dark signal.

The raw signal of the radiometer  $I(n)$  for the  $n$ -th pixel is recorded in digital counts [22]. The total number of pixels (spectral channels), ADC output format and range of gains and integration times are instrument-specific parameters. Wavelength scale of the radiometer given as a function of pixel number  $n = (1 \dots 256)$  has been provided by manufacturer in the calibration certificate of the radiometer and will not be verified during LCE-2. The respective dark signal  $S_{c0}(\lambda)$  is subtracted, and the signal is divided by the spectral irradiance from the certificate of the lamp  $E(\lambda, l_0)$  interpolated to the designated wavelength,  $\lambda(n)$ :

$$R_E(\lambda) = \frac{(S_c(\lambda) - S_{c0}(\lambda)) C_{\text{stray}} C_{\text{temp}} C_{\text{lin}}}{E(\lambda, l_0) G_c}, \quad (2)$$

where  $G_c$  is the gain amplification factor of the radiometer, if used at different gains. Correction for the stray light  $C_{\text{stray}}$  is estimated from a spectral stray light correction matrix of the spectrometer if available; additionally, corrections to account for temperature affecting the instrument responsivity,  $C_{\text{temp}}$ , and for instrument linearity,  $C_{\text{lin}}$  have to be estimated, if the instrument is used at different temperatures and/or at different signal levels during calibration and application. For calibration conditions  $C_{\text{lin}}$  and  $C_{\text{temp}}$  usually are taken equal to 1.

To derive the irradiance  $E(\lambda)$  [mW m<sup>-2</sup> nm<sup>-1</sup>] the determined spectral irradiance responsivities  $R_E(\lambda)$  have to be applied to subsequent radiometric field measurements  $S(\lambda)$  as

$$E(\lambda) = \frac{(S(\lambda) - S_0(\lambda)) C_{\text{stray}} C_{\text{temp}} C_{\text{lin}}}{R_E(\lambda) G_c}, \quad (3)$$

where  $S_0(\lambda)$  are the instrument's dark signal responses determined in the field. In the field measurements (3) the corrections for nonlinearity and for ambient temperature may be much more relevant than in (2).

#### 6.1.2 Spectral Radiance Calibrations

Radiance responsivity calibrations require a uniform Lambertian source of known radiance that will fill the angular field of view (FOV) of the radiance sensor. Most frequently two calibration procedures are used [16], [17]: radiance calibrations by using a reflectance plaque and radiance calibrations by using an integrating sphere.







In the case of first procedure for determination of spectral radiance responsivity of the radiometer, the radiation from a calibrated diffuse reflectance plaque is measured. The plaque is illuminated by a calibrated lamp of known spectral irradiance, placed at the fixed distance of at least 500 mm from the plaque. Baffles with small apertures are placed between the lamp and the diffuser to reduce the stray light. The radiance input optics of the radiometer is placed at view angle  $45^\circ$  from normal in front of the diffuser plaque at a distance of several centimetres, allowing the FOV to be filled by reflected radiation. In this case for calculation of responsivity  $R_L(\lambda)$ , the reflected radiance  $L(\lambda)$  is used instead of spectral irradiance  $E(\lambda, l_0)$  from the calibration certificate of the lamp as in expression (1). Reflected radiance  $L(\lambda)$  is expressed by:

$$L(\lambda) = \frac{E(\lambda, l_0)}{\pi} R(0^\circ, 45^\circ, \lambda). \quad (4)$$

Here  $R(0^\circ, 45^\circ, \lambda)$  is the bidirectional reflectance factor of the diffuser plate taken from the calibration certificate and interpolated to designated wavelength  $\lambda$ .

If a radiance sensor at a lamp distance of 500 mm from the plaque is saturated or in the case of large FOV of the radiance sensor, the distance between the lamp and diffuser should be increased similarly to procedure of equation (1).

In the case of second procedure for calibrating spectral radiance sensors the radiation from a uniformly illuminated integrating sphere is measured. An exit port of the sphere should be large enough to completely fill the sensor's FOV. The target port of the sphere must be large enough to place the sensor so far away that reflections off the sensor's entrance optics will not go significantly back into the sphere. If the sensor is too close, the reflected light can increase the intensity and distort the uniformity of the radiance distribution within the sphere. The spectral radiance scale of an integrating sphere source is determined by comparison with the spectral irradiance scale of a standard lamp.

The spectral irradiance  $E(\lambda, d, r_1, r_2)$  of the integrating sphere's exit port is measured using the irradiance scale transfer radiometer. The signal  $S(\lambda)$  and respective dark signal  $S_0(\lambda)$  are recorded with the source exit port open and covered, and source irradiance  $E(\lambda, d, r_1, r_2)$  is calculated using (3).

Assuming a uniform radiance distribution within the sphere's exit port, the spectral radiance scale of the integrating sphere is calculated as

$$L(\lambda) = \frac{E(\lambda, d, r_1, r_2)[d^2 + r_1^2 + r_2^2]}{\pi r_1^2} [1 + \delta + \delta^2 + \dots], \quad (5)$$

where  $r_1$  is the radius of the circular source aperture,  $r_2$  is the radius of the detector aperture,  $d$  is the distance between the apertures, and  $\delta = r_1^2 r_2^2 (d^2 + r_1^2 + r_2^2)^{-2}$ .

In either approach, the radiance responsivity calibration coefficients  $R_L(\lambda)$  of the field radiometer are determined as

$$R_L(\lambda) = \frac{(S_r(\lambda) - S_{r0}(\lambda)) C_{\text{stray}} C_{\text{temp}} C_{\text{lin}}}{L(\lambda) G_c}, \quad (6)$$

where  $S_r(\lambda)$  is the signal measured with the radiance sensor directed to the center of the source aperture, and  $S_{r0}(\lambda)$  is the respective dark signal.

To derive the radiance  $L(\lambda)$  [ $\text{mW m}^{-2} \text{nm}^{-1} \text{sr}^{-1}$ ] the determined spectral radiance responsivities  $R_L(\lambda)$  have to be applied to subsequent radiometric field measurements  $S_r(\lambda)$  as

$$L(\lambda) = \frac{(S_r(\lambda) - S_{r0}(\lambda)) C_{\text{stray}} C_{\text{temp}} C_{\text{lin}}}{R_L(\lambda) G_c}. \quad (7)$$





## 6.2 Tests before radiometric calibrations

### 6.2.1 Radiance sensor's FOV and response of cosine collectors

Although radiometric calibration coefficients of a radiance sensor do not depend directly on the FOV of the sensor, the FOV must be known for properly setting up the sensor for calibration as the FOV must be uniformly filled during radiometric calibration. In addition, during OC field measurements anisotropic targets such as sky and water are measured and depending on illumination and view configurations the results measured with instruments having different FOV might not be directly comparable.

For determining the FOV of a radiance sensor the device under test is placed on a rotation stage with the rotation axis lying in the plane and crossing the center of the entrance aperture of the radiometer. A stable small light source is placed several metres in front of the radiometer. The FOV is scanned with smaller angular increments in the region of rapid change of responsivity at the wings of the FOV and larger increments elsewhere. The increment size should be chosen so that possible change of responsivity within the FOV and full width at half maximum (FWHM) of the FOV could be determined. 10 measurements inside the FOV and 10 measurements at both wings of the FOV could be a reasonable choice. The measurements should begin and end with the light source at the optical axis of the radiometer for checking the stability of the source. Alternatively a separate monitor detector can be used for verifying the stability of the lamp.

The entrance optics of an irradiance sensor must provide angular response corresponding to cosine function. Deviation from cosine function can be checked with similar setup as used for measuring the FOV of a radiance sensor. At first the spectrum with the sensor looking straight into the calibration source is recorded. The  $\theta = 0^\circ$  alignment should place the centre of the cosine collector on the axis of illumination, with the collector surface oriented normal to the axis. For that an alignment laser beam intersecting with the filament of the lamp is aimed at the centre of the collector. The position of the radiometer is adjusted until a mirror held flat against the cosine collector reflects the laser beam back on itself. The rotational scale is zeroed in this position. The laser beam should remain in the centre of the collector when the test instrument is rotated between the angles from  $0^\circ$  to  $90^\circ$ , and the laser beam should just graze the collector's surface at the  $\theta = 90^\circ$  incidence angle. In testing directional response of cosine collectors the sensor is rotated in the range  $0^\circ$  to  $90^\circ$  in both rotating directions with  $\leq 5^\circ$  increments at smaller incidence angles and  $\leq 1^\circ$  increments at  $\theta > 80^\circ$ . The accuracy of angle positioning should be at least  $0.1^\circ$ . The measurements are normalized with response of the radiometer at  $\theta = 0^\circ$ , therefore, measurements at normal incidence should be repeated or a separate monitor detector must be used for the lamp. During the measurements the surface of the cosine collector must be uniformly illuminated.

### 6.2.2 Polarization sensitivity

Polarization sensitivity of above-water radiance instruments has to be tested before radiometric calibrations, and sensitivity to linear polarization less than 2% is acceptable. The tested radiometer is placed according to the measurement scheme in chapter 6.1.2 at  $45^\circ$  angle on the calibration table in the rotator mount ensuring that the tested instrument could be freely rotated through  $360^\circ$  around its optical axis. At first radiance data without polarizer are recorded in  $2^\circ$  steps over  $360^\circ$ . Then immediately in front of the tested radiometer the polarizer is placed, and after alignment the polarized data are recorded with increment of  $2^\circ$  over a full  $360^\circ$  rotation of the tested sensor.

### 6.2.3 Non-linearity effects

The linearity of the radiometric channels should be determined over the whole range of use if different signal levels during calibration and application are expected.

The values are to be normalized at the gain setting used during absolute calibration that is for the integration time at which the spectrometer was calibrated, see  $G_c$  for (2) and (6).

Nonlinearity of gain settings can vary with both wavelength and integration time [23]. Since the spectral power distribution of the test and calibration source may be different, it is advisable to use the test source for the actual nonlinearity measurement of the spectrometer if applicable.

For certain types of radiometers (TriOS RAMSES, Satlantic HyperOCR) the non-linearity effect due to different integration times can be corrected to 0.1 %, if at least two spectra measured with different integration times are available. Spectrum  $S_{1,2}(\lambda)$  corrected for nonlinearity is calculated by using the following formula:

$$S_{1,2}(\lambda) = \left[ 1 - \left( \frac{S_2(\lambda)}{S_1(\lambda)} - 1 \right) \left( \frac{1}{t_2/t_1 - 1} \right) \right] S_1(\lambda). \quad (8)$$

Here  $S_1(\lambda)$  and  $S_2(\lambda)$  are the initial spectra measured with integration times  $t_1$  and  $t_2$ . Minimal ratio usually is  $t_2/t_1 = 2$ , but it may be also 4, 8, 16, etc. For large ratios  $t_2/t_1 > 8$  the spectrum  $S_1(\lambda)$  is close to corrected spectrum  $S_{1,2}(\lambda)$  and application of (8) is not needed.

Usually the nonlinearity of the spectrometer gain settings over its spectral range is determined, defined as the relative difference between the actual integration time and that displayed by the spectrometer.

#### 6.2.4 Spectral stray light

When a monochromatic source is measured with a spectrometer, the recorded signal normalized to one is called *spectral line spread function* (LSF) [24], [25]. LSF describes the relative responsivity of each detector array element of the spectrometer to excitation at this particular wavelength. LSFs measured at the central wavelength of every array element of the spectrometer form a *spectral stray light matrix* (SLM). SLM is a square matrix which rows are LSFs, columns of the SLM are *slit-scattering functions* (SSF) [26]. SSF describes the relative spectral responsivities of different spectral bands of the spectrometer. The measured value recorded by a single spectral band is convolution of the optical input signal with the SSF corresponding to that band. When the full SLM of a spectrometer is known, the stray light can be removed from the measured spectrum and the 'true' source spectrum can be restored. This can be done also in the case of the broad-band signals measured from natural objects.

Correction of bandpass and stray light effects can be done by mathematical operation called a spectral deconvolution. Unfortunately, the deconvolution of measured spectra due to noise of the measured signal and/or in the estimated SLM may give unstable results. Therefore, existing correction algorithms of measured spectra often deal with the problem of the stray light or of the bandpass separately, and for getting stable solution different regularisation procedures modifying the SLM are applied. From literature, several deconvolution algorithms can be found, based on either iterative approach [26]–[28] or inverse matrix multiplication proposed by Zong e.a. [18], [22], [24], [25], [29], [30]. A number of techniques dealing only with the bandpass correction are available [31]–[34]. Lately a method for the simultaneous correction of bandpass and stray light effects also has been proposed by Nevas e.a [35].

At TO a special study for characterisation of the OCR radiometers for quantification of the effect of stray light and comparison of possible methods for its correction is in progress [5], [6]. In order to apply stray light corrections the individual SLM should be available for each particular spectrometer. Determination of SLM is time consuming and for all instruments participating in comparisons not possible in the time frame of LCE-2.

#### 6.2.5 Ambient temperature

Calibration measurements are usually made in a temperature controlled environment. The array spectroradiometers used for field measurements are used over the temperature range from 2 °C to 35 °C, thus can be affected by various temperature effects, which certainly can increase the measurement uncertainty. Therefore, each instrument should be individually tested and characterized for temperature effects at least in the range from 5 °C to 35 °C. Results are usually presented relative to the instrument's response at 20 °C.

Thermal effects can be reliably quantified only in stable conditions. In general, the internal temperature of the tested instrument is lagged behind the ambient temperature. As relaxation after a temperature change depends on the type of spectroradiometer, knowledge of stabilisation time of the particular instrument is important for successful performance of field measurements. Usually the influence of temperature on the dark signal and responsivity of the radiometer are tested. Ambient temperature can

affect also the wavelength positions or cause distortions of the slit function of spectroradiometer restricting the reliable use of instrument for field measurements [36].

Commonly the temperatures cited above are environmental temperatures, but it should be noted that any correction should rather use the temperature of the affected element, which is normally inside the instrument. Thus, the instruments equipped with temperature sensors placed at critical locations within the instrument may be preferable for critical applications. For highest precision, dynamic temperature testing involving temporal transients, as well as possible temperature gradients within an instrument, may be appropriate. For temperature correction the internal temperature of the instrument is preferred to the instantaneous ambient temperature.

### 6.3 Uncertainty contributions for laboratory calibrations and tests

The uncertainty is calculated [37] from the contributions originating from the spectral irradiance of the standard lamp, including data from the calibration certificate, from interpolation of the spectral irradiance values to the designated wavelengths, from instability of the lamp due to working time elapsed after calibration, from contribution to the spectral irradiance due to setting and measurement of the current of the lamp, from measurement of the distance between the lamp and input aperture of the radiometer, from the spatial uniformity of the irradiance at 500 mm distance, and from reproducibility of the alignment. For the array spectroradiometer uncertainty contributions arising from dark measurements, from repeatability and reproducibility of measurements are included. For input quantities relative standard uncertainties are estimated. The relative combined standard uncertainty of output quantity is calculated by combining relative standard uncertainty of each input estimate by using formula (12) of [15]. Uncertainty of final result is given as relative expanded uncertainty with a coverage factor  $k = 2$ . Current uncertainty estimates may be subject to changes during LCE-2 project implementation.

To minimize the effect of random noise in the measured spectrum, a large number of spectrometer signals are averaged. It is advisable that the number of recorded spectra in series  $n$  and the number of repeated series  $N$  were the same for all quantities measured. The same averaging for all signals, and for the ambient background and/or for the instrument's dark responses recorded with different integration times may cause longer recording durations, but it will standardize the Type A uncertainty estimates and make their combining more reliable.

#### 6.3.1 Calibration certificate of the standard lamp

Uncertainty stated in the certificate of reference standard lamp usually gives a dominating contribution to the combined uncertainty estimate. Table 1 presents an overview of uncertainties reported by manufacturers, and by some metrology institutes. Present uncertainty estimate of FEL irradiance standard used by Tartu Observatory is 0.6 % from 430 nm to 900 nm.

Table 1: Standard uncertainties stated by different calibration service providers for standard lamps.

Company & lamp type	Wavelength $\lambda$ /nm	Standard uncertainty $u$ /%
Oriel Ins., Osram Sylvania FEL 1000 W, T6	250	1.9
	350	1.4
	654.6	1.35
	900	1.4
	1300	1.45
MIKES, Osram Sylvania FEL 1000 W, T6	290 - 310	1.4 - 0.95
	320 - 380	0.85
	390 - 400	0.8
	410 - 900	0.6
NPL, UK, FEL 1000 W	250 - 290	0.9
	300 - 410	0.8 - 0.6
	420 - 560	0.5 - 0.4
	570 - 770	0.35
	780 - 1200	0.25 - 0.5



### 6.3.2 Lamp ageing

The irradiance produced by a standard lamp changes with burning time. Ageing during a simulated use cycle of pre-selected, pre-aged modified FEL lamps is described in [12]–[14]. The continuous drift after seasoning for 60 hours of the new FEL lamps from Osram Sylvania measured at 300 nm is reported to be less than 0.01 % in hour [38]. However, stepwise changes in the radiation output of these lamps (up to  $\pm 1$  %) may occur at unpredictable intervals. Therefore, it is advisable to have at least three standard lamps ready for use, and system allowing regular stability checking of the lamps.

Present uncertainty estimate due to lamp ageing is 0.6 % after 50 hours. Thus, for a lamp with 40 hours working time:

$$u_{12} = \frac{0,6 \%}{\sqrt{3}} \frac{40}{50} = 0.28 \%$$

### 6.3.3 Interpolation

Calibration laboratories usually provide calibration points at 5 nm to 20 nm intervals. For interpolation between these points, different equations are recommended. Spectral irradiance values calculated by using these equations have an additional uncertainty of up to 0.5 %. However, some calibration labs including MIKES provide interpolation formulas both for irradiance and for uncertainty, and have this contribution already included to their combined uncertainty estimate.

Present uncertainty estimate due to interpolation: 0.2 %.

### 6.3.4 Lamp current and shunt

For operation of standard FEL lamps, among the most critical parameters is the lamp current. According to [26], [38] the percentage change in the current of lamp will cause approximately  $5 \times (600/\lambda)$  times the percentage change in spectral irradiance. Effect of lamp current offset was checked for the lamps used at TO. Results are shown in Fig. 10. Three spectra were measured, one with nominal current of 8.200 A, and two with current deviating  $\pm 50$  mA from nominal. The results of Figure 13 agree well with the estimate proposed in [26]. The inversely proportional dependence of uncertainty on the wavelength is evident.

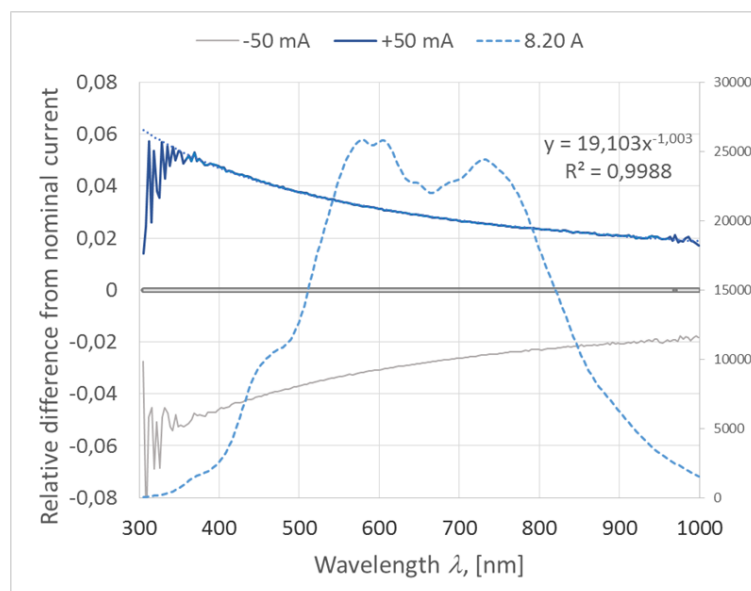


Figure 13: Effect of lamp current offset measured at TO.

Present uncertainty estimate due to shunt used for the measurement of the lamp current is 0.002 %. The uncertainty due to lamp current, if standard uncertainty of the current is 1 mA, is calculated as



$$u_{cu} = \frac{38}{\lambda} \%$$

if the wavelength is presented in [nm].

### 6.3.5 Diffuse reflectance plaque (certificate, correction if needed)

In calibration certificate of the diffuse reflectance standard diffuse directional-hemispherical reflectance  $\rho(8^\circ/H)$  in the range from 300 nm to 1750 nm with standard uncertainty less than 0.2 % is specified. Comparison of measured values of bidirectional reflectance factor  $R(0^\circ/45^\circ)$  with directional-hemispherical spectral reflectance  $\rho(6^\circ/H)$  for pressed PTFE, gave in the spectral interval from 400 nm to 1600 nm for the ratio  $R(0^\circ/45^\circ)/\rho(6^\circ/H)$  values between 1.02 and 1.025 [39]–[41]. Applying this correction to the values stated in the calibration certificate lead to an additional uncertainty in radiance of about 0.2 %. Present estimate for uncertainty of radiance due to reflectance plaque including certificate and additional correction is 0.3 % for the plaque used by Tartu Observatory.

### 6.3.6 Distance

Distance between the reference planes of the lamp and entrance optics of the radiometer, measured along the optical axis (x-axis) is also very important parameter. The reference plane of the lamp is specified in the calibration certificate. The front surface of the lamp socket is commonly used as the reference. At the usual distance of 500 mm the lamp can be regarded as a point source, therefore, irradiance changes with distance according to the inverse square law, and a 1 mm error in distance will cause a 0.4 % error in irradiance.

Additional calibration uncertainty may be introduced by the geometry of the radiometer's entrance optics. If a quartz window is used to protect the input optics, the optical path of the incident radiation is reduced by refraction, which e.g. for a 2.5 mm plate is 0.8 mm [38]. Present estimate if the distance of 500 mm is measured with standard uncertainty of 0.2 mm, then uncertainty of irradiance due to distance measurement is 0.08 %. For larger distances (about 1 m) the uncertainty of irradiance due to distance measurement is 0.12 %.

### 6.3.7 Reproducibility of adjustment (lamp, plaque, sensor)

Alignment errors of the lamp across optical axis less than  $\pm 1$  mm in the y or z directions (cf. Figure 14), rotation of the lamp around x and z axes less than  $\pm 0.1^\circ$ , and around y axes less than  $2^\circ$  will cause uncertainty in the irradiance less than 0.1 % [38]. Positioning errors of the input optics of the radiometer lead to an additional irradiance uncertainty of about 0.1 %. Alignment errors concerning the diffusing plaque lead to an additional uncertainty of radiance about 0.1 %. This accuracy can be achieved only by very careful alignment by means of special adjustment laser.

Present estimate for alignment: due to lamp 0.1 %; due to radiometer 0.1 %; due to plaque 0.1 %.

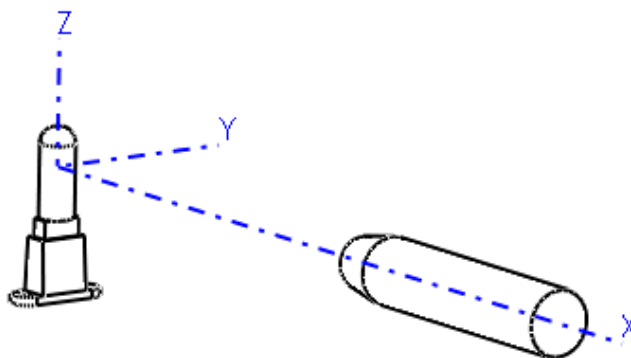


Figure 14: Coordinate system of irradiance calibration setup.

### 6.3.8 Random effects (repeatability of spectra, and dark signal)

Present estimate for standard uncertainty due to random effects in the spectral region from 400 nm to 900 nm is less than 0.1 %.

### 6.3.9 Environmental effects (temperature)

When calibrating array spectroradiometers with silicon detectors, the present estimate for standard uncertainty due to temperature variability in the spectral region from 400 nm to 700 nm is around 0.1 %, and will increase up to 0.6 % for longer wavelengths (950 nm).

### 6.3.10 Non-linearity effects

According to specifications of the instrument performance in [17] the non-linearity effects should be correctable to less than 0.1 %. For some hyperspectral radiometers, spectra measured at different integration times and brought to the same scale by using respective gain factors show relative differences up to 3 %. This difference depends on the measured signal level with respect to the possible extreme indication, and is largest close to this maximum value. This means that even if only the results measured at the same integration time are compared, the systematic bias is still present if the signal levels in different labs were somewhat different. The formula (8) developed for non-linearity correction has been successfully checked for significantly differing signal levels, and it performs satisfactorily in the spectral region from 400 nm to 900 nm causing additional uncertainty for corrected spectrum around 0.1 %. Outside this region, the uncertainty is rapidly increasing. Present estimate for standard uncertainty due to non-linearity correction is 0.1 %.

### 6.3.11 Combined standard uncertainty

Relative standard uncertainty for calibration of irradiance sensors together with relative uncertainties of input quantities is shown in Figure 15 and in Table 2 for selected wavelengths of the Sentinel 3 Ocean and Land Colour Instrument (OLCI).



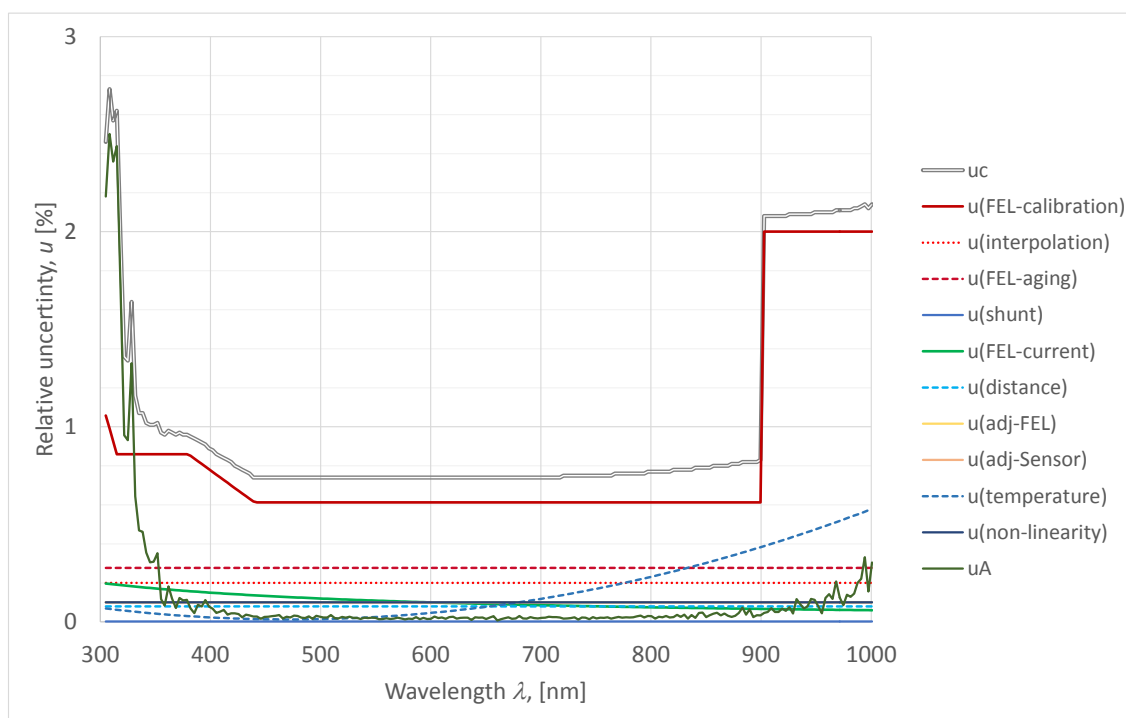


Figure 15: Relative standard uncertainty for calibration of irradiance sensors.

Table 2: Calibration uncertainty budget of irradiance sensors.

Uncertainty components	Selected spectral bands of the Sentinel 3 OLCI sensor					
	400 nm	442.5 nm	490 nm	560 nm	665 nm	778.8 nm
FEL standard lamp irradiance	0.78 %	0.61 %	0.61 %	0.61 %	0.61 %	0.61 %
Interpolation of irradiance	0.2 %	0.2 %	0.2 %	0.2 %	0.2 %	0.2 %
Lamp ageing	0.28 %	0.28 %	0.28 %	0.28 %	0.28 %	0.28 %
Shunt	0.002 %	0.002 %	0.002 %	0.002 %	0.002 %	0.002 %
Lamp current	0.15 %	0.14 %	0.12 %	0.11 %	0.09 %	0.08 %
Distance lamp - sensor	0.08 %	0.08 %	0.08 %	0.08 %	0.08 %	0.08 %
Alignment of lamp position	0.1 %	0.1 %	0.1 %	0.1 %	0.1 %	0.1 %
Alignment of radiometer	0.1 %	0.1 %	0.1 %	0.1 %	0.1 %	0.1 %
Temperature variability	0.03 %	0.02 %	0.02 %	0.03 %	0.09 %	0.2 %
Non-linearity correction	0.1 %	0.1 %	0.1 %	0.1 %	0.1 %	0.1 %
Repeatability including dark signal	0.08 %	0.03 %	0.03 %	0.02 %	0.02 %	0.03 %
Combined standard uncertainty	0.88 %	0.74 %	0.74 %	0.74 %	0.74 %	0.76 %
Expanded uncertainty, $k=2$	1.8 %	1.5 %	1.5 %	1.5 %	1.5 %	1.5 %



Relative standard uncertainty for calibration of radiance sensors together with relative uncertainties of input quantities is shown in Figure 16 and in Table 3 for selected wavelengths of the Sentinel 3 OLCI.

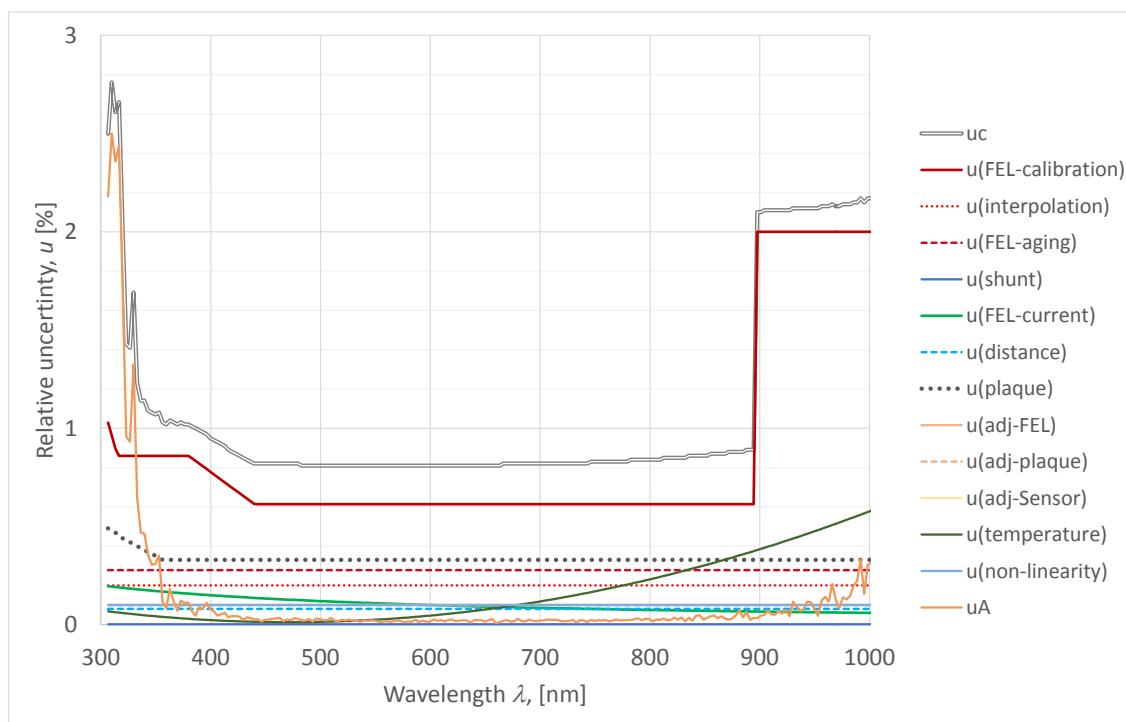


Figure 16: Relative standard uncertainty for calibration of radiance sensors.

Table 3: Calibration uncertainty budget of radiance sensors.

Uncertainty components	Selected spectral bands of the Sentinel 3 OLCI sensor					
	400 nm	442.5 nm	490 nm	560 nm	665 nm	778.8 nm
FEL standard lamp irradiance	0.78 %	0.61 %	0.61 %	0.61 %	0.61 %	0.61 %
Interpolation of irradiance	0.2 %	0.2 %	0.2 %	0.2 %	0.2 %	0.2 %
Lamp aging	0.28 %	0.28 %	0.28 %	0.28 %	0.28 %	0.28 %
Shunt	0.002 %	0.002 %	0.002 %	0.002 %	0.002 %	0.002 %
Lamp current	0.15 %	0.14 %	0.12 %	0.11 %	0.09 %	0.08 %
Distance lamp - sensor	0.08 %	0.08 %	0.08 %	0.08 %	0.08 %	0.08 %
Plaque refl. factor $R(0^\circ/45^\circ)$	0.33 %	0.33 %	0.33 %	0.33 %	0.33 %	0.33 %
Alignment of lamp position	0.1 %	0.1 %	0.1 %	0.1 %	0.1 %	0.1 %
Alignment of radiometer	0.1 %	0.1 %	0.1 %	0.1 %	0.1 %	0.1 %
Alignment of plaque position	0.1 %	0.1 %	0.1 %	0.1 %	0.1 %	0.1 %
Temperature variations	0.03 %	0.02 %	0.02 %	0.03 %	0.09 %	0.2 %
Non-linearity correction	0.1 %	0.1 %	0.1 %	0.1 %	0.1 %	0.1 %
Repeatability including dark signal	0.08 %	0.03 %	0.03 %	0.02 %	0.02 %	0.03 %
Combined stand. uncertainty	0.95 %	0.82 %	0.81 %	0.81 %	0.81 %	0.83 %
Expanded uncertainty, $k=2$	1.9 %	1.6 %	1.6 %	1.6 %	1.6 %	1.7 %





## 6.4 Indoor measurements

Correction for the stray light,  $C_{\text{stray}}$ , for temperature affecting the instrument responsivity,  $C_{\text{temp}}$ , and for instrument linearity,  $C_{\text{lin}}$ , used in the formulas (2), (3), (6) and (7) are calculated according to the specific conditions prevailing during the measurements. As radiometric calibrations are made in a temperature controlled environment and using only one integration time, corrections  $C_{\text{lin}}$  and  $C_{\text{temp}}$  are often taken equal to 1. For the field measurements according to (3) and (7), the corrections for nonlinearity and for ambient temperature may be much more relevant. The stray light correction  $C_{\text{stray}}$ , if available, should be applied to every measured spectrum, not only to the field measurements but also when the standard lamp is measured for the responsivity calibration of the instrument.

## 6.5 Outdoor measurements

Two outdoor exercises are planned for LCE-2. For primary outdoor exercise all the radiometers are fixed to a common frame and aligned by a single key operator to measure approximately the same sky or water surface area. All acquisitions are strictly synchronised. For secondary outdoor exercise all the participants set up and operate their instruments themselves and acquisitions are loosely synchronised.

During the primary outdoor exercise [42] [43], [44], the basic quantities subject to comparison will be irradiance and radiance of natural objects (i.e. sky and water surface). Thus, in the case of similar input optics, the indoor measurement equations (3) and (7) will apply. Main differences are related to the greater temporal and spatial variability of the natural objects compared to the laboratory ones (requires better synchronization between the instruments) and the fact that light coming from sky and water surface is partially polarized [45].

In the case of secondary outdoor exercise, radiometers will be operated in their regular configuration to derive water-leaving radiance  $L_w$  [46]:

$$L_w(\lambda) = L_u(\lambda) - \rho(w_s)L_d(\lambda), \quad (9)$$

where

$L_u$  is measured upwelling radiance (including sky glint);

$L_d$  is measured downwelling (sky) radiance;

$\rho(w_s)$  is factor describing surface specular reflection depending on the wind speed  $w_s$  [47] :

$$\rho(w_s) = 0.0256 + 0.00039w_s + 0.000034w_s^2 \quad \text{for} \quad \frac{L_d(\lambda=750)}{E_s(\lambda=750)} < 0.05 \quad (10)$$

and

$$\rho(w_s) = 0.0256 \quad \text{for} \quad \frac{L_d(\lambda=750)}{E_s(\lambda=750)} \geq 0.05. \quad (11)$$

Remote sensing reflectance is derived from  $L_w$  [43]:

$$R_{RS} = \frac{L_w(\lambda)}{E_d(\lambda)}, \quad (12)$$

where  $E_d$  is measured global downwelling (direct + diffuse) irradiance. The measured irradiance and radiance values are handled in the same manner as in 6.4.

Because of different view geometries of instruments and setups participating in the intercomparison,  $L_w$  and  $R_{RS}$  should be normalized to zenith sun or to nadir viewing angle before comparison as follows [48]–[50]:

$$L_{wn}(\lambda) = L_w(\lambda) \frac{\mathfrak{R}_0}{\mathfrak{R}(\theta', w_s)} \frac{\frac{f_0(\lambda, \tau_a, Chl)}{Q_0(\lambda, \tau_a, Chl)}}{\frac{f(\lambda, \tau_a, Chl, \theta_s, \theta', \Delta\phi)}{Q(\lambda, \tau_a, Chl, \theta_s, \theta', \Delta\phi)}}. \quad (13)$$

$\mathfrak{R}(\theta', w_s)$  is geometrical factor accounting for multiple reflections and refractions at the air-water interface,  $\theta'$  is a refracted view zenith angle



$$\theta' = \arcsin\left(\frac{\sin \theta_v}{n}\right), \quad (14)$$

where  $\theta_v$  is the view zenith angle and  $n$  is the refractive index of water. Values of  $\Re(\theta', w_s)$  are tabulated in [51] and  $\Re_0 = \Re(\theta' = 0, w_s = 0)$ .

$f(\lambda, \tau_a, Chl, \theta_s, \theta', \Delta\phi)$  binds reflectance to the inherent optical properties (IOP) of water and  $Q(\lambda, \tau_a, Chl, \theta_s, \theta', \Delta\phi)$  describes the bidirectional characteristics of the reflectance.

Here  $\tau_a(\lambda)$  is the atmospheric aerosol optical thickness;

$Chl$  is chlorophyll- $a$  concentration;

$\theta_s$  is the solar zenith angle;

$\Delta\phi$  is the relative azimuth angle between solar and viewing directions;

$f_0()$  and  $Q_0()$  are normalized values of  $f()$  and  $Q()$ , respectively, i.e. where  $\theta_s = \theta_v = 0$ .

Parameter  $f/Q$  is tabulated in [52]. Re-calculation for the particular waterbody might be needed.

## 6.6 Uncertainty budgets for comparison measurements

Uncertainty analysis is made for two indoor and four outdoor measurement tasks. In laboratory, comparison of irradiance sensors measuring FEL reference standard in Table 6, and comparison of radiance sensors measuring integrating sphere in Table 7. In tables 6 to 9 uncertainty estimation is based on experimental data of TriOS RAMSES sensors and information in [1], [43], [44], [53], [54].

Table 4: Uncertainty budget of indoor measurements: irradiance sensors measuring FEL.

Uncertainty components	Selected spectral bands of the Sentinel 3 OLCI sensor					
	400 nm	442.5 nm	490 nm	560 nm	665 nm	778.8 nm
Absolute calibration	1 %	0.8 %	0.8 %	0.8 %	0.8 %	0.8 %
Responsivity change	0.5 %	0.3 %	0.3 %	0.3 %	0.5 %	0.7 %
Environmental effects (radiometer)	0.03 %	0.02 %	0.02 %	0.03 %	0.09 %	0.2 %
Comparison source (FEL)	0.5 %	0.5 %	0.5 %	0.5 %	0.5 %	0.5 %
Combined standard uncertainty	1.2 %	1 %	1 %	1 %	1.1 %	1.2 %
Expanded uncertainty, $k=2$	2.4 %	2 %	2 %	2 %	2.2 %	2.4 %

Table 5: Uncertainty budget of indoor measurements: radiance sensors measuring integrating sphere.

Uncertainty components	Selected spectral bands of the Sentinel 3 OLCI sensor					
	400 nm	442.5 nm	490 nm	560 nm	665 nm	778.8 nm
Absolute calibration	1.4 %	1.2 %	1.2 %	1.2 %	1.2 %	1.2 %
Responsivity change	0.5 %	0.3 %	0.3 %	0.3 %	0.5 %	0.7 %
Environmental effects (radiometer)	0.03 %	0.02 %	0.02 %	0.03 %	0.09 %	0.2 %
Comp. source (integrating sphere)	0.5 %	0.5 %	0.5 %	0.5 %	0.5 %	0.5 %
Combined standard uncertainty	1.2 %	1.1 %	1.1 %	1.1 %	1.1 %	1.3 %
Expanded uncertainty, $k=2$	2.4 %	2.2 %	2.2 %	2.2 %	2.2 %	2.6 %

Outdoor uncertainty is analysed for four measurement tasks: comparison of irradiance sensors measuring global downwelling irradiance  $E_d$  in Table 6, comparison of radiance sensors measuring upwelling radiance  $L_u$  in Table 7, comparison of radiance sensors measuring downwelling radiance  $L_d$  in 8, and comparison of the three radiometer systems used for determination of remote sensing

reflectance  $R_{RS}(\lambda)$  in 9. Uncertainty estimation is based on experimental data of TriOS RAMSES sensors and information in [1], [43], [44], [53], [54].

Table 6: Uncertainty budget of irradiance sensors measuring global downwelling irradiance  $E_d$ .

Uncertainty components	Selected spectral bands of the Sentinel 3 OLCI sensor					
	400 nm	442.5 nm	490 nm	560 nm	665 nm	778.8 nm
Absolute calibration	1.2 %	1 %	1 %	1 %	1 %	1 %
Responsivity change	0.7 %	0.5 %	0.5 %	0.5 %	0.7 %	1 %
Environmental effects (radiometer)	1 %	1 %	1 %	1 %	1.2 %	2 %
Non-cosine response	1 %	1 %	1 %	1 %	1 %	1 %
Viewing angle correction	1.5 %	1.5 %	1.5 %	1.5 %	1.5 %	1.5 %
Environmental effects (measurand)	1 %	1 %	1 %	1 %	1 %	1 %
Combined standard uncertainty	2.5 %	2.4 %	2.4 %	2.4 %	2.5 %	3.2 %
Expanded uncertainty, $k=2$	5 %	4.8 %	4.8 %	4.8 %	5 %	6.4 %

Table 7: Uncertainty budget of radiance sensors measuring upwelling radiance  $L_u$ .

Uncertainty components	Selected spectral bands of the Sentinel 3 OLCI sensor					
	400 nm	442.5 nm	490 nm	560 nm	665 nm	778.8 nm
Absolute calibration	1.4 %	1.2 %	1.2 %	1.2 %	1.2 %	1.2 %
Responsivity change	0.5 %	0.3 %	0.3 %	0.3 %	0.5 %	0.7 %
Environmental effects (radiometer)	1 %	1 %	1 %	1 %	1.2 %	2 %
Non-cosine response	1 %	1 %	1 %	1 %	1 %	1 %
Viewing angle correction	1.5 %	1.5 %	1.5 %	1.5 %	1.5 %	1.5 %
Environmental effects (measurand)	2 %	2 %	2 %	2 %	3 %	4 %
Combined standard uncertainty	3 %	2.8 %	2.8 %	2.8 %	3.7 %	4.9 %
Expanded uncertainty, $k=2$	6 %	5.6 %	5.6 %	5.6 %	7.4 %	9.8 %

Table 8: Uncertainty budget of radiance sensors measuring downwelling radiance  $L_d$ .

Uncertainty components	Selected spectral bands of the Sentinel 3 OLCI sensor					
	400 nm	442.5 nm	490 nm	560 nm	665 nm	778.8 nm
Absolute calibration	1.4 %	1.2 %	1.2 %	1.2 %	1.2 %	1.2 %
Responsivity change	0.5 %	0.3 %	0.3 %	0.3 %	0.5 %	0.7 %
Environmental effects (radiometer)	1 %	1 %	1 %	1 %	1.2 %	2 %
Non-cosine response	1 %	1 %	1 %	1 %	1 %	1 %
Viewing angle correction	1.5 %	1.5 %	1.5 %	1.5 %	1.5 %	1.5 %
Environmental effects (measurand)	2 %	2 %	2 %	2 %	3 %	4 %
Combined standard uncertainty	3 %	2.8 %	2.8 %	2.8 %	3.7 %	4.9 %
Expanded uncertainty, $k=2$	6 %	5.6 %	5.6 %	5.6 %	7.4 %	9.8 %

Table 9 Uncertainty budget for three sensors system determining remote sensing reflectance  $R_{RS}(\lambda)$ .

Uncertainty components	Selected spectral bands of the Sentinel 3 OLCI sensor					
	400 nm	442.5 nm	490 nm	560 nm	665 nm	778.8 nm
System calibration	2 %	2 %	2 %	2 %	2 %	2 %
Responsivity change	0.5 %	0.3 %	0.3 %	0.3 %	0.5 %	0.7 %
Environmental effects (radiometer)	1 %	1 %	1 %	1 %	1.2 %	2 %
Non-cosine response	1 %	1 %	1 %	1 %	1 %	1 %
Stray light correction	2 %	0.5 %	0.5 %	0.5 %	0.5 %	1 %
Polarization correction	1 %	1 %	1 %	1 %	1 %	1 %
Viewing angle correction	1.5 %	1.5 %	1.5 %	1.5 %	1.5 %	1.5 %
Environmental effects (measurand)	2 %	1.5 %	1.5 %	1.5 %	1.5 %	2 %
Combined standard uncertainty	4.1 %	3.3 %	3.3 %	3.3 %	3.4 %	4.2 %
Expanded uncertainty, $k=2$	8.2 %	6.6 %	6.6 %	6.6 %	6.8 %	8.4 %

The considered uncertainty sources of 9 are the following. At first, uncertainty of the three-radiometer system calibration determined assuming the same irradiance standard is used for the calibration of the  $E_d$ ,  $L_u$ , and  $L_d$  sensors [37]. So system calibration accounts for mechanical alignments of lamps, plaques and sensors, inadequate baffling, short time instability of irradiance standard, and uncertainty of diffuse reflectance plaque.

## 7 Measurement instructions

In this chapter, the measurement procedure for both the indoor and outdoor comparison exercises will be described [45]. Considering the SI traceability of remote sensing results, these exercises are logically placed between the laboratory calibration and the actual fieldwork in order to help in detecting and quantifying of the error sources.

The indoor and outdoor comparison exercises follow directly the responsivity calibration of the participating radiometers in the TO's optical laboratory and the calibration results will be made available to the users.

### 7.1 Indoor comparison

The indoor intercomparison is meant to be performed by the owner/operator of the radiometer under supervision of the laboratory staff. The light sources, power supplies, and monitoring devices are provided by TO and the measurement setup will be prepared considering the stable laboratory conditions. Because of the cleanroom requirements, all instruments brought into laboratory area should be carefully cleaned by the TO's personnel. It is possible to use TO's computers for instrument control and recording of results to reduce the organizing overhead, assuming that the necessary software is available before the comparison exercise. Internal clocks of the related instruments (including computers) should be synchronized before the measurements.

Two measurement setups will be prepared, one for intercomparison of irradiance sensors according to (2) and other for intercomparison of radiance sensors according to (6). The measurement setups are established in separate rooms and may be operated simultaneously reducing the total time needed for participants to perform all the measurements. The measurement geometry is shown in Figure 17. Maintaining the suitable laboratory environment and providing equipment needed for intercomparison, monitoring the stability, and alignment of radiometers subject to comparison is responsibility of TO's personnel while practical setting up of the radiometer and collecting measurement data in accordance with comparison guidelines is responsibility of the radiometer's operator. A short checklist with all the necessary actions in the right order is provided in comparison guidelines (Appendix C).

#### 7.1.1 Irradiance sensors

For irradiance sensors, a calibrated 1000 W tungsten halogen (FEL) source is used. The lamp setup and monitoring is described in Chapter 4.2.1. The setup of the indoor irradiance comparison is shown in Figure 17.

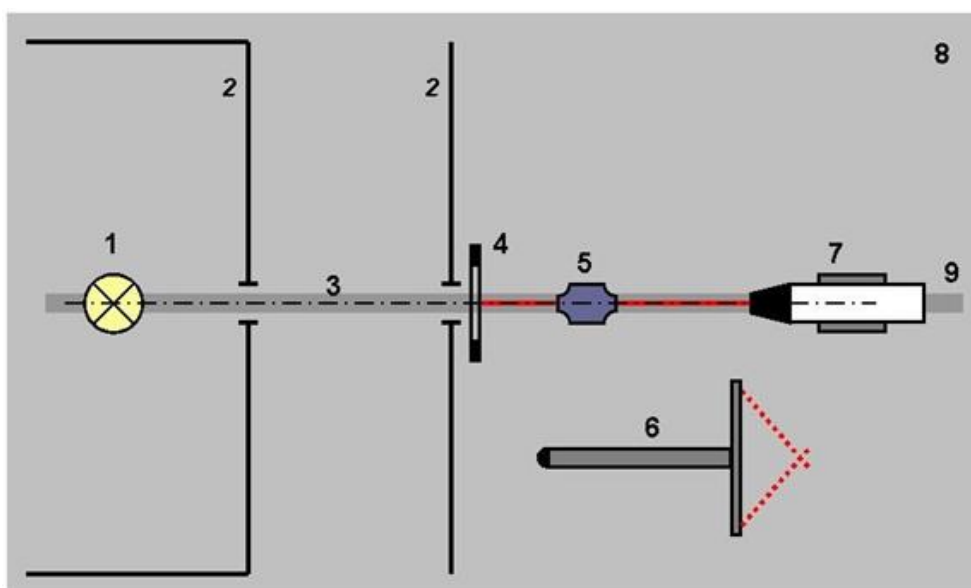


Figure 17: Indoor irradiance comparison. 1 - FEL lamp; 2 - baffles; 3 - main optical axis; 4 - alignment jig; 5 - alignment laser; 6 - distance tool; 7 - radiometer on the support; 8 - optical table; 9 - optical rail.

The irradiance sensor is placed horizontally on the optical axis at a certain distance from the light source, defined by a special target jig. The distance between the lamp and radiometer will be approximately 1 m. The exact value of spectral irradiance is determined by using a standard radiometer according to (1) and corrected by the monitor sensor. The lamp and the target jig are aligned before comparison measurements explicitly by TO's personnel. The participant will have a platform on the optical rail with all the necessary adjustment elements and with a set of clamps to fix the instrument. Participant will adjust the distance between the radiometer and the target jig to be exactly 500 mm by using the special distance tool provided by TO. All cables should be connected to the radiometer and radiometer powered on at least 30 minutes before the measurements.

The user will set up the radiometer as follows:

- 1) connect all the necessary cables and power on the radiometer
- 2) install the temporary dual-beam alignment laser;
- 3) install radiometer under comparison using any of the supports available;
- 4) position the centre of the cosine collector along the laser beam
- 5) rotate and tilt the radiometer to be parallel to the optical axis
- 6) set up the distance between alignment jig and radiometer using a special tool
- 7) repeat steps 4)..6) until no further adjustments are needed.

After the final alignment is approved by the TO's supervisor, the data should be collected as follows:

- 1) the radiometer readings acquired in series of 30 readings;
- 2) at least three sets of series separated by no less than one minute interval;
- 3) the readings should be, whenever possible, taken at three different manually controlled integration times. The longest integration time should be chosen to align the raw signal maximum close (but not exceeding) the saturation level; the other two integration times approximately 2 and 4 times shorter;
- 4) each recorded value will be equipped with timestamp, integration time and any necessary metadata;
- 5) recording of the raw data (preferably in human-readable text files) is obligatory; storing of the derived irradiance values is up to the user.

It is possible, within the time frame, to re-align the radiometer for testing the repeatability and rotate the radiometer around its optical axis in order to take into account the properties of the cosine corrector and inherent optical system.

### 7.1.2 Radiance sensors

For radiance sensors, an integrating sphere with internal quartz tungsten halogen source is used. The sphere source is described in Chapter 4.2.2, equations (4), (5) and (6). Scheme of the setup for the indoor radiance comparison is shown in Figure 18.

The sphere source is operated explicitly by TO's personnel. The user will be provided with a mechanical platform for mounting the radiometer with all the necessary adjustment elements and a set of clamps to fix the position of the instrument. All cables should be connected to the radiometer and radiometer powered on at least 30 minutes before the measurements.

The user should align the radiometer along the optical axis crossing the centre of the sphere's output port as follows:

- 1) connect all the necessary cables and power on the radiometer
- 2) the sensor's input window is aligned symmetrically in both the vertical and horizontal directions;
- 3) distance between the sensor and the sphere is chosen so that the diameter of the output port exceeds the one determined by sensor's FOV by at least a factor of two;
- 4) after proper alignment, minor adjustments of the sensor in any direction should not change the raw output signal.



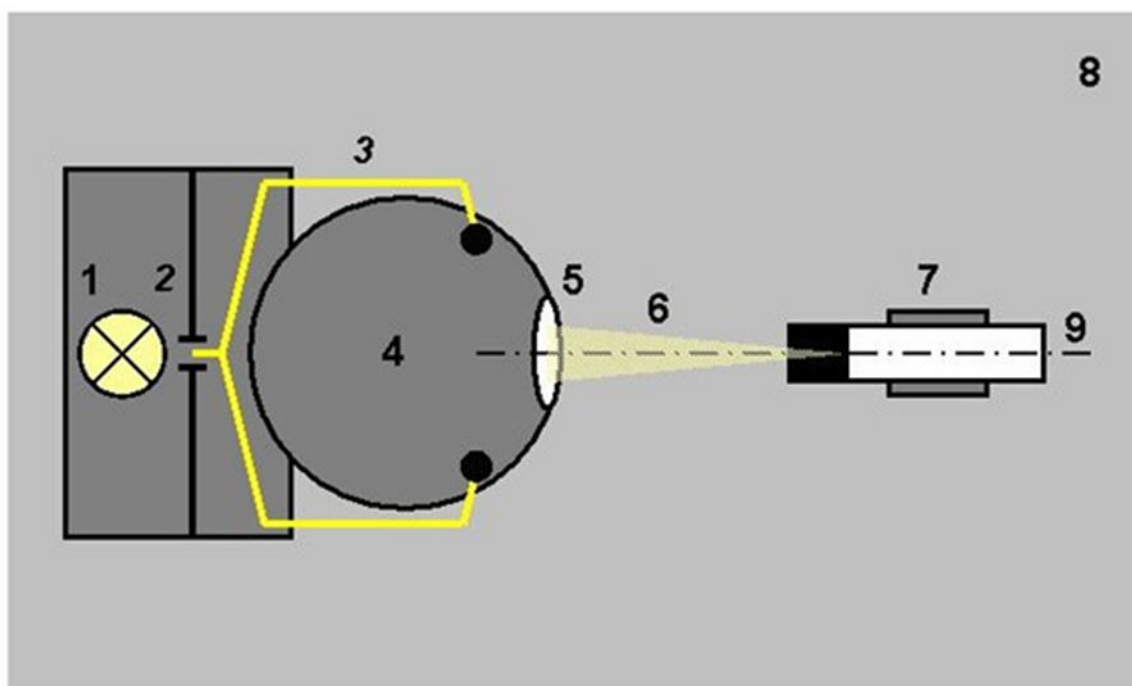


Figure 18: Indoor radiance comparison. 1 - quartz tungsten halogen lamp; 2 - variable slit; 3 - optical fibre; 4 - integrating sphere; 5 - output port; 6 - FOV of the radiometer; 7 - radiometer on the support; 8 - optical table; 9 - main optical axis.

After the final alignment is approved by the TO's supervisor, the data should be collected as described in the previous chapter. The radiance sensors are operated at two source intensities to simulate the different conditions comparable to sky and water radiance levels. The source intensity is adjusted by TO's personnel and monitored by a silicon sensor attached to the sphere. It is possible, within the time frame, to re-align the radiometer for testing the experiment's repeatability.

## 7.2 Outdoor comparison

The main purpose of the outdoor comparison is to establish link between the laboratory and field measurements. Two types of outdoor exercises are planned. Priority is given to the primary comparison where all instruments are pointed to the same physical object and data are acquired synchronously. The instruments in this case will be operated by a single key person while the data is collected by instrument owners/operators. The primary comparison is planned on the first day of the outdoor exercises keeping the second day for spare. During the second phase of outdoor comparison, each participant is setting up his/her full measurement setup, pointing to the collectively agreed direction and collecting data during the sparsely defined time frame.

### 7.2.1 The primary outdoor comparison

In order to eliminate as much as possible the temporal and spatial variability of the natural sources, all radiometers will be tied together to measure approximately the same area of sky or water surface and the data collection will be strictly synchronized. The physical quantities selected for the comparison exercise are absolute spectral irradiance and radiance. The measurement site is described in Chapter 4.3. The radiometers will be set up by TO's personnel based on the information gathered from the users in the earlier phases of this project. The prepared frames will fit all the previously described instruments from the registered participants while last minute changes are not guaranteed. The frame will ensure parallelism of optical axes for all the attached radiometers and the absence of shadowing of each other in the case of the irradiance sensors. The manually controlled rotating platform allowing quick change of the sensor azimuth and elevation angles will be provided by TO. The radiometers will be operated on the upper platform of the tower.

Responsibility of the participants will be:

- 1) setting up computers and any necessary devices on the lower platform of the tower;
- 2) routing and attaching the instrument cables;
- 3) synchronizing internal clocks of computers and instruments to the UTC;
- 4) ensuring that all instruments are in operating condition and batteries fully charged;
- 5) preparing the controlling software for data acquisition with short notification time;
- 6) preparing logbook for instant measurement data.

Instrument gains and integration times should be selected according to the usual fieldwork practice. Data acquisition is started and finished and the station names announced by the key person operating the instrument frame.

Collecting of the data depends on the weather conditions, but the measurement plan is following:

- 1) measurement geometry is selected by the key person;
- 2) station name/number is announced by the key person;
- 3) station start command is announced by the key person;
- 4) timestamp is logged and the acquisition of all instruments started by the participants;
- 5) measurement conditions are constantly logged by all participants;
- 6) station stop command is announced by the key person;
- 7) timestamp is logged and the acquisition of all instruments stopped by the participants.

Typical duration of a station will be 30 seconds. The stations can be cancelled afterwards considering the weather/object conditions or technical issues. Environmental parameters, water samples, and metadata will be collected by TO's personnel but can be duplicated by the participants if not disturbing the comparison exercise. The measurement sessions will be announced by the key person.

The following terms apply to the data acquisition and are on the responsibility of the participants:

- 1) each recorded value will be equipped with timestamp, integration time, and any necessary metadata;
- 2) recording of the raw values (preferably in human readable text files) is obligatory; storing of the calculated results is up to the user.

Data processing should follow the guidelines in Chapter 8. Participants will provide both the raw data files and calibrated/filtered/averaged results on per-station basis.

Final analysis of comparison results will be carried out by TO, the supposed primary quantities are [43], [44]:

- 1) absolute spectral radiance (upwelling and downwelling);
- 2) downwelling global absolute spectral irradiance;

In order to assess the different FOV-s of the radiance sensors, a derived quantity such as nadir corrected water leaving radiance should be used instead of upwelling and downwelling radiances.

### 7.2.2 The secondary outdoor comparison

During the secondary outdoor comparison, each participant is responsible to set up both the radiometers (using their usual fieldwork configuration) and the logging equipment. The radiometers will be set up according to the TR8 ("Protocols and Procedures for Field Inter-Comparisons of Fiducial Reference Measurement (FRM) Field Ocean Colour Radiometers (OCR) used for Satellite Validation") of the current project. As an example, the measurement setup with three TriOS RAMSES instruments is shown in Figure 19.

Measurement directions and time frames will be collectively agreed during the exercise while each participant is responsible to collect all the data (if supported by the instruments) needed for comparison of the following physical quantities [43], [44]:

- 1) water-leaving absolute spectral radiance;
- 2) downwelling global absolute spectral irradiance;
- 3) remote sensing reflectance of water.





Collecting of the weather and metadata (except water samples) is on the participants' responsibility as well.

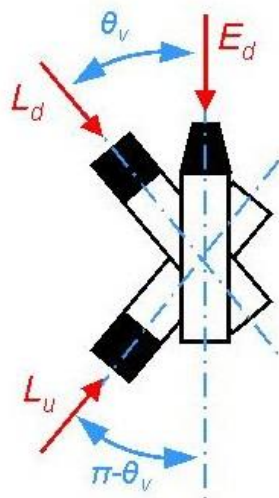


Figure 19 Proposed reflectance measurement setup.



## 8 Calculations and data processing

The purpose of data processing is to give directions to the users to derive the required quantities, namely absolute spectral irradiance and radiance, using collected raw data, laboratory calibration data and unified algorithms. During all measurements, both in the laboratory and field conditions, the users are encouraged to record the raw instrument data (raw pixel readings, timestamp, signals from the pressure/depth and temperature sensors and so on). Storing the raw data together with the device's calibration history is considered the optimal way to obtain reliable measurement results. In the scope of the comparison exercises, calibration data for all the participating radiometers will be maintained by TO.

### 8.1 Instrument data processing

The general guidelines for all types of instruments are described here while a detailed example is given in Appendix B. Whenever possible, sensor raw data (e.g. ADC readings) should be stored as the measurement result. If supported by the controlling software, plain text files are preferred.

As in general, these steps in the following order are needed to retrieve irradiance/irradiance values in physical units:

- 1) subtraction of the dark/background signal
- 2) linearity correction
- 3) stray light correction
- 4) wavelength scale/bandpass correction
- 5) applying normalized integration time
- 6) applying radiometric calibration coefficients
- 7) applying thermal correction coefficients

While not all the corrections are applicable/reasonable for all the instruments, points 1) and 6) are needed as minimum to retrieve the calibrated result. This processing chain should be applied to each raw measurement before any further statistical analysis. As an exception, the outliers are allowed to be removed from the raw dataset before processing if the physical reason can be clearly determined. Based on the corrected and calibrated results, arithmetic average and standard deviation for each series should be calculated.

The following quantities for each series should be calculated by the user and will serve as input for the comparison exercise:

- 1) start and end time
- 2) arithmetic mean value
- 3) standard deviation
- 4) number of acquisitions
- 5) number of discarded acquisitions

### 8.2 Intercomparison

The final analysis of intercomparison results will be carried out by TO. For that, users should provide the collected data - raw data files - and final calibration results, averaged over all valid series recorded, and corrected for significant systematic effects together with relevant uncertainty estimates. The weighted mean of participants would be a preferred reference value [2], [3], if a consistency check by applying a chi-squared test will show a satisfactory agreement between participants. Otherwise the median [4] as largely insensitive to the existence of outliers will be used.

### 8.3 Data processing example: TriOS RAMSES hyperspectral radiometers

The radiance and irradiance sensors of the TriOS RAMSES family share similar data flow. Each instrument has 256 pixels at fixed wavelengths, about 18 masked pixels to account for the temperature drifts, fixed signal gain, a 16-bit ADC and integration time associated with each spectrum. The integration times can be selected manually or using autoprobe in the range of (4..8192) ms. Each device is equipped with a unique serial number.

Factory or calibration facility provided device files contain following information necessary for raw data processing (see Appendix A):

- 1) polynomial coefficients binding pixel number to the wavelength;
- 2) dark\_start and dark\_stop corresponding to the masked pixels;
- 3) back1 and back2 for each pixel to restore the dark signal non-uniformity;
- 4) cal for each pixel, the radiometric responsivity coefficient.

Spectra are recorded in the plain text files (storing into database is implemented as well) containing header with some metadata (instrument's serial number, timestamp, comments, integration time) and columns containing pixel number and ADC raw count. In the first data row (corresponding to the pixel 0), the integration time is coded.

The factory proposed data processing method, covering only the dark signal subtraction and radiometric calibration, is following (see Appendix B for numerical example):

- 1) normalize the raw signal (divide all pixel values by 0xFFFF=65535);
- 2) subtract from pixel values back1 and scaled with integration time back2;
- 3) find average value of the masked pixels and subtract from all pixel values;
- 4) scale all pixel values to 8192 ms and divide by cal to get the calibrated result.

In this simplified schema, thermal effects (except the dark signal drift determined by the masked pixels), non-linearity, bandwidth and stray light are not taken into account, neither is evaluated the measurement uncertainty.

## 8.4 Uncertainty evaluation

The uncertainty analysis has been carried out according to the ISO Guide to the Expression of Uncertainty in Measurement [15], and to the EA guide EA 4/02. Evaluation is based on the measurement model, which describes the output quantity  $y$  as a function  $f$  of input quantities  $x_i$ :  $y = f(x_1, x_2, x_3 \dots)$ . For every input quantity standard uncertainty is evaluated separately. There are two types of standard uncertainties: Type A is of statistical origin; Type B is determined by other means. Both types of uncertainties are indicated as standard deviation, denoted correspondingly by  $s$  and  $u$ . In calibration of array spectrometers, the uncertainty contributions arising from averaging of a large number of repeatedly measured spectrums is considered as of Type A. Contributions from calibration certificates (lamp, current shunt, multimeter, diffuse reflectance panel etc.), but also from instability and spatial non-uniformity of the lamp are considered of Type B.

## 9 Reporting of results

Results of the radiometric calibration will be made available by TO to the participants before the indoor comparison exercise. These instant results depend on the instrument type and are, in general, released in the form of device files recognisable by dedicated software that will be used to operate the instruments during the indoor and outdoor comparison exercises. The complete calibration certificates will be released later.

Measurement conditions (environmental, parameters of the waterbody etc.) will be recorded by TO and released to the participants as soon as possible. Example of the station protocol for the outdoor comparison is shown in Appendix.

Collecting, storing, processing and reporting of the instrument data from the indoor and outdoor comparisons is the responsibility of the participants. Both the raw and calibrated/corrected/averaged data should be made available to TO. Calibrated data will be used for the "blind" intercomparison while the raw data is necessary to assess various correction schemes and to detect for possible data processing issues. As a general requirement for the intercomparison, all calibrated/calculated data should include corresponding measurement uncertainties. Guidelines for evaluation of the uncertainties will be given in the final version of this document.

### 9.1 Indoor comparison

During the indoor comparison, absolute spectral irradiance and radiance of the known stable sources will be measured by the participants under the supervision of TO-s personnel. Averaged values of irradiance/radiance values, standard uncertainties, the start/end times and number of measurements for each series serve as the primary inputs for the intercomparison. TO will provide irradiance/radiance values of the source together with uncertainty estimates for any given measurement series referring to the timestamps, these values will serve as reference values for the indoor comparison.

### 9.2 Outdoor comparison

The primary outdoor intercomparison follows the ideology of the indoor comparison and requirements for the reported results are similar. Results of the secondary outdoor comparison will include both the spectral irradiance/radiance values and derived quantities such as  $L_w$ ,  $R_{rs}$ , depending on the measurement geometry. The participants should report all the measured (calibrated) and calculated results together with uncertainties. Detailed report depends on the specific method and instruments used in the comparison. Reference values for the outdoor comparison will be determined as the weighted mean of all specific type results reported by participants, if a consistency check will show a satisfactory agreement. Otherwise the median of all reported results will be used as reference.



## 10 Recommendations

### 10.1 Introduction

There are currently a few approaches available to consider for the quality improvement and in-field calibration assurance in the framework of FRM OCR. Amongst them are

- field intercomparison campaigns, using currently available instruments and best practices for planning of comparisons, calibrating the instruments, performing the field measurements, collecting and processing the data;
- developing a novel standard radiometer, key parameters of which are better in comparison with the existing instruments by a factor of 3...5;
- developing a novel field calibration unit for monitoring the stability of the field radiometers between calibrations in the laboratory.

### 10.2 Intercomparison

Field intercomparison, supported by laboratory calibration and characterisation of the participating instruments, has been one of the main methods to ensure the quality and useability range of the field results [1], [37], [55]. While not always truly a SI-traceable measurement, the intercomparison would give valuable information about the instruments' stability and outdoor performance. In most cases, the radiometers are set up in the stable field conditions using tight geometry and illumination constraints, still trying to mimic the real field conditions (Figure 20).



Figure 20: The intercalibration bench used in the frame of the BOUSSOLE project [55].

The participating radiometers are calibrated against SI-traceable standards just before or after the field campaign, presumably by a single lab to further reduce variability between participants due to different calibration sources.

Expanded version of such intercomparison will be carried out during LCE-2 of the current project, and described in the previous chapters of this document. The intercomparison is organised as a chain between SI-traceable laboratory calibration and the real field experiment. The chain contains five vital links in the following order:

- Calibration of the laboratory standards against primary standards of a leading NMI
- Laboratory calibration of all participating field instruments
- Indoor intercomparison measuring stable sources under supervision of dedicated laboratory staff
- Outdoor intercomparison with strictly supervised measurement geometry
- Outdoor intercomparison by using individual geometry and procedures of participants under typical environmental conditions.





After every step, the data will be analysed by the pilot laboratory, and NMI will supervise the whole process in particular supporting the evaluation of uncertainties. Such step-by-step intercomparison should establish a stronger link between the field results and SI units, and point to the bottlenecks, where improvement of the instruments and methodologies is most critically needed.

### 10.3 Reference radiometer

In recent years, standard radiometers have been developed in many related fields, including atmospheric remote sensing [56], [57] and ocean colour [58].

One major objective of the QASUME project [56], [57] was to reduce the uncertainties of atmospheric spectral UV measurements in order to be able to detect long-term changes in terrestrial solar radiation. QASUME is a traveling spectroradiometer, consisting of a double scanning monochromator, a specially designed entrance optics, a wavelength calibration lamp, a temperature-controlled box, power supplies and data acquisition system (Figure 21). Traceability of the QASUME system has been validated during several campaigns, including radiometric calibration against the primary standard of spectral irradiance (the blackbody) at NMI. For the solar UV irradiance, standard uncertainty below 0.5% was achieved for the wavelength range of (300...500) nm.



Figure 21: The traveling spectroradiometer QASUME installed at El Arenosillo, Spain [59].

MOBY (The Marine Optical Buoy) is a set of ocean color radiometers maintained by NASA and dedicated to support satellite remote sensing since the SeaWiFS project. Recently, a project was initiated to improve the characteristics of the instrumentation to meet the high requirements for the fiducial calibration facilities. The improvements include, amongst others, renewing the spectroradiometer's optical system to have better spectral resolution, higher SNR and lower stray light level. The scheduled end of the project is in 2019. Improving of the optical and radiometric parameters (Figure 22) is achieved by using spectrometer module of novel design, already available from number of manufacturers. Experience collected during the MOBY-Refresh project [58] would be helpful considering the possible development of a traveling standard radiometer for FRM OCR.

A well characterised portable standard radiometer would support FRM OCR in the cases of stationary measurement stations [60] as well as during field intercomparison events. According to the experience gathered during the last two decades, main restrictions of the miniature field radiometers are related to

- radiometric sensitivity (SNR),
- stability of the radiometric calibration,
- radiometric linearity,
- spectral stray light,
- bandwidth,
- dark signal uncertainty,
- temperature coefficients.



Improvement of these parameters is a feasible task, considering the current state of the optoelectrical industry. Most attention should be paid to the metrological assurance of such instrument, to the measurement protocols, data interpretation and availability.

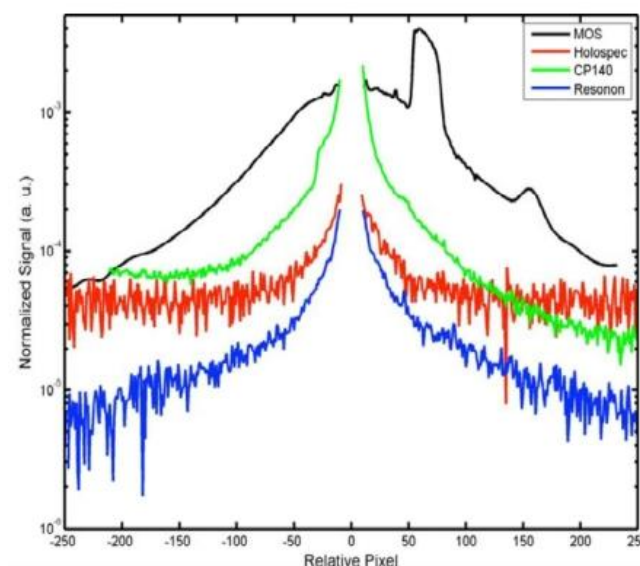


Figure 22: Improved stray light characteristics of the MOBY-Refresh [58].

#### 10.4 Field calibration unit

In addition to the traveling standard radiometer, a well characterised stable, portable calibration unit would be vital support to the FRM OCR activities. The portable calibrator can be used in the case of stationary or remote measurement systems, where other calibration methods are unavailable. During the field intercomparisons, the portable calibrator help to bind the radiometric scales of all participating instruments between each-other and to the SI units. Considering the price and technical difficulties, development and maintenance of a field calibration unit meeting the OC requirements and being suitable for most types of field radiometers, is comparable to the challenges related to the possible development of a standard radiometer. Figure 23 shows the TriOS FieldCAL insatrumet, allowing to check the temporal stability of the RAMSES radiance and irradiance sensors [61].



Figure 23: The TriOS FieldCAL portable calibration unit [61].

## 11 Conclusions

This document provides base guidelines for organising the Laboratory Comparison Exercise LCE-2. The purpose of the LCE-2 is to review critically the methodologies used by teams to practically verify the calibration of FRM OCR using external reference SI traceable calibration sources, and document protocols and best practice for it. The LCE-2 also serves as a preparation stage for the FICE-AAOT field intercomparison exercise. The LCE 2 can be divided into three sub-tasks:

- 1) SI-traceable radiometric calibration of participating radiometers;
- 2) Indoor intercomparison in controlled environment;
- 3) Outdoor intercomparison over terrestrial water surface.

During the indoor intercomparison, the method of direct comparison against stable reference standard is proposed. During the outdoor intercomparison, a reference value will be combined from concurrently measured values obtained by using freshly calibrated OCR instruments of participants. The intercomparison results will be analysed by TO.

The participating radiometers are calibrated against SI-traceable standards just before the field campaign at TO in order to reduce possible variability between participants due to different calibration sources. The intercomparison is organised as a chain between SI-traceable laboratory calibration and the real field experiments. The chain contains five links in the following order:

- Calibration of the reference standards of TO against primary standards of a leading NMI;
- Radiometric calibration of all participating field instruments at TO;
- Indoor intercomparison measuring stable sources under supervision of dedicated staff;
- Outdoor intercomparison with strictly specified measurement geometry;
- Outdoor intercomparison by using individual geometry and procedures of participants under typical environmental conditions.

After every step, the data will be analysed by the pilot laboratory, and NMI will supervise the whole process supporting in particular the evaluation of uncertainties. Such step-by-step intercomparison should establish a stronger link between the field results and SI units, and point to the bottlenecks, where improvement of the instrumentation and methodologies is most critically needed.

LCE-2 links the OC field measurements to the SI-traceable calibration and verifies whether different instruments measuring the same object can provide consistent results within the stated uncertainty limits. LCE-2 is organized as a five-step chain between SI-traceable laboratory calibration and the real field experiments. In this way, LCE-2 reveals most critical problems presently affecting consistency of field experiments.

## 12 References

- [1] G. Zibordi *et al.*, "In situ determination of the remote sensing reflectance: an inter-comparison," *Ocean Sci.*, vol. 8, pp. 567–586, 2012.
- [2] M. G. Cox, "The evaluation of key comparison data," *Metrologia*, vol. 39, no. 6, p. 589, 2002.
- [3] G. Ratel, "Median and weighted median as estimators for the key comparison reference value (KCRV)," *Metrologia*, vol. 43, no. 4, p. S244, 2006.
- [4] J. W. Müller, "Possible Advantages of a Robust Evaluation of Comparisons," *J. Res. Natl. Inst. Stand. Technol.*, vol. 105, no. 4, pp. 551–555, 2000.
- [5] I. Ansko, J. Kuusk, and R. Vendt, "MERIS Validation and Algorithm 4th reprocessing – MERIS Validation Team (MVT)," Tartu Observatory, Tõravere, INTERMEDIATE REPORT No. 1, May 2015.
- [6] I. Ansko, J. Kuusk, R. Vendt, and V. Vabson, "MERIS Validation and Algorithm 4th reprocessing – MERIS Validation Team (MVT)," Tartu Observatory, Tõravere, INTERMEDIATE REPORT No. 2, May 2016.
- [7] C. J. Lorenzen, "Determination of Chlorophyll and Pheo-Pigments: Spectrophotometric Equations<sup>1</sup>," *Limnol. Oceanogr.*, vol. 12, no. 2, pp. 343–346, Apr. 1967.
- [8] H. Utermöhl, "Zur Vervollkommnung der quantitativen phytoplankton-methodik," *Mitteilungen Int. Ver. Theor. Angew. Limnol.*, vol. 9, pp. 1–38, 1958.
- [9] S. Tassan and G. M. Ferrari, "An alternative approach to absorption measurements of aquatic particles retained on filters," *Limnol. Oceanogr.*, vol. 40, no. 8, pp. 1358–1368, Dec. 1995.
- [10] J. E. Tyler, "The secchi disc," *Limnol. Oceanogr.*, vol. 13, no. 1, pp. 1–6, 1968.
- [11] "BIPM, IEC, IFCC, ILAC, ISO, IUPAC, IUPAP and OIML, International Vocabulary of Metrology—Basic and General Concepts and Associated Terms (VIM), JCGM 200:2008, Aug. 2011."
- [12] N. J. Harrison, E. R. Woolliams, and N. P. Fox, "Evaluation of spectral irradiance transfer standards," *Metrologia*, vol. 37, no. 5, p. 453, 2000.
- [13] J. Hartmann, "Advanced comparator method for measuring ultra-small aperture areas," *Meas. Sci. Technol.*, vol. 12, no. 10, p. 1678, 2001.
- [14] Y. Ohno and J. K. Jackson, "Characterization of modified FEL quartz-halogen lamps for photometric standards," *Metrologia*, vol. 32, no. 6, p. 693, 1995.
- [15] "Guide to the Expression of Uncertainty in Measurement." International Organization for Standardization (ISO), Geneva-1995.
- [16] B. Carol Johnson, H. Yoon, J. P. Rice, and A. C. Parr, "Chapter 1.2 - Principles of Optical Radiometry and Measurement Uncertainty," in *Experimental Methods in the Physical Sciences*, vol. 47, C. J. D. and A. C. P. Giuseppe Zibordi, Ed. Academic Press, 2014, pp. 13–67.
- [17] J. L. Mueller, G. S. Fargion, and C. R. McClain, Eds., "Ocean optics protocols for satellite ocean color sensor validation: Instrument specifications, characterization, and calibration." NASA/TM-2003-21621/Rev-Vol II, 2003.
- [18] S. G. R. Salim, N. P. Fox, W. S. Hartree, E. R. Woolliams, T. Sun, and K. T. V. Grattan, "Stray light correction for diode-array-based spectrometers using a monochromator," *Appl. Opt.*, vol. 50, no. 26, pp. 5130–5138, Sep. 2011.
- [19] S. G. R. Salim, E. R. Woolliams, and N. P. Fox, "Calibration of a Photodiode Array Spectrometer Against the Copper Point," *Int. J. Thermophys.*, vol. 35, no. 3–4, pp. 504–515, May 2014.
- [20] L. Ylianttila, R. Visuri, L. Huurto, and K. Jokela, "Evaluation of a Single-monochromator Diode Array Spectroradiometer for Sunbed UV-radiation Measurements<sup>¶</sup>," *Photochem. Photobiol.*, vol. 81, no. 2, pp. 333–341, Mar. 2005.
- [21] G. Seckmeyer, "Instruments to Measure Solar Ultraviolet Radiation Part 4: Array Spectroradiometers (lead author: G. Seckmeyer) (WMO/TD No. 1538). 44 pp. November 2010." WMO, 2010.
- [22] M. Talone, G. Zibordi, I. Ansko, A. C. Banks, and J. Kuusk, "Stray light effects in above-water remote-sensing reflectance from hyperspectral radiometers," *Appl. Opt.*, vol. 55, no. 15, pp. 3966–3977, May 2016.
- [23] S. G. R. Salim, N. P. Fox, E. Theocharous, T. Sun, and K. T. V. Grattan, "Temperature and nonlinearity corrections for a photodiode array spectrometer used in the field," *Appl. Opt.*, vol. 50, no. 6, pp. 866–875, Feb. 2011.
- [24] Y. Zong, S. W. Brown, B. C. Johnson, K. R. Lykke, and Y. Ohno, "Simple spectral stray light correction method for array spectroradiometers," *Appl. Opt.*, vol. 45, no. 6, pp. 1111–1119, Feb. 2006.
- [25] Y. Zong, S. W. Brown, G. Meister, R. A. Barnes, and K. R. Lykke, "Characterization and correction of stray light in optical instruments," 2007, vol. 6744, p. 67441L–67441L–11.
- [26] Kostkowski, *Reliable Spectroradiometry*. Spectroradiometry Consulting, 1997.
- [27] S. W. Brown *et al.*, "Stray-light correction algorithm for spectrographs," *Metrologia*, vol. 40, no. 1, p. S81, 2003.
- [28] H. Slaper, H. a. J. M. Reinen, M. Blumthaler, M. Huber, and F. Kuik, "Comparing ground-level spectrally resolved solar UV measurements using various instruments: A technique resolving effects of wavelength shift and slit width," *Geophys. Res. Lett.*, vol. 22, no. 20, pp. 2721–2724, Oct. 1995.
- [29] M. E. Feinholz *et al.*, "Stray Light Correction of the Marine Optical System," *J. Atmospheric Ocean. Technol.*, vol. 26, no. 1, pp. 57–73, Jan. 2009.
- [30] A. Barlier-Salsi, "Stray light correction on array spectroradiometers for optical radiation risk assessment in the workplace," *J. Radiol. Prot.*, vol. 34, no. 4, p. 915, 2014.
- [31] E. I. Stearns and R. E. Stearns, "An example of a method for correcting radiance data for Bandpass error," *Color Res. Appl.*, vol. 13, no. 4, pp. 257–259, Aug. 1988.

- [32] Y. Ohno, "A flexible bandpass correction method for spectrometers," in *Proc. AIC Colour 05–10th Congress of the Int. Colour Association*, Grenada, Spain, 2005.
- [33] E. R. Woolliams, R. Baribeau, A. Bialek, and M. G. Cox, "Spectrometer bandwidth correction for generalized bandpass functions," *Metrologia*, vol. 48, no. 3, p. 164, 2011.
- [34] S. Eichstädt *et al.*, "Comparison of the Richardson–Lucy method and a classical approach for spectrometer bandpass correction," *Metrologia*, vol. 50, no. 2, p. 107, 2013.
- [35] S. Nevas, G. Wübbeler, A. Sperling, C. Elster, and A. Teuber, "Simultaneous correction of bandpass and stray-light effects in array spectroradiometer data," *Metrologia*, vol. 49, no. 2, p. S43, 2012.
- [36] L. L. A. Price, R. J. Hooke, and M. Khazova, "Effects of ambient temperature on the performance of CCD array spectroradiometers and practical implications for field measurements," *J. Radiol. Prot.*, vol. 34, no. 3, p. 655, 2014.
- [37] S. B. Hooker *et al.*, "The Seventh SeaWiFS Intercalibration Round-Robin Experiment (SIRREX-7), TM-2003-206892, vol. 17, NASA Goddard Space Flight Center, Greenbelt," Feb. 2002.
- [38] G. Bernhard and G. Seckmeyer, "Uncertainty of measurements of spectral solar UV irradiance," *J. Geophys. Res. Atmospheres*, vol. 104, no. D12, pp. 14321–14345, Jun. 1999.
- [39] B. C. Johnson, H. Yoon, J. P. Rice, and A. C. Parr, "Chapter 1.2 - Principles of Optical Radiometry and Measurement Uncertainty," in *Optical Radiometry for Ocean Climate Measurements*, Elsevier, 2014.
- [40] H. W. Yoon, D. W. Allen, G. P. Eppeldauer, and B. K. Tsai, "The extension of the NIST BRDF scale from 1100 nm to 2500 nm," in *Proc. SPIE 7452, Earth Observing Systems XIV*, 2009, vol. 7452, p. 745204–1 to 12.
- [41] M. E. Nadal and P. Y. Barnes, "Near infrared 45 degrees/o degrees reflectance factor of pressed polytetrafluoroethylene (PTFE) powder," *J. Res. Natl. Inst. Stand. Technol.*, vol. 104, no. 2, p. 185, Mar. 1999.
- [42] "MERIS Optical Measurement Protocols Part A: In-situ water reflectance measurements, CO-SCI-ARG-TN-008 Issue 2.0." ESA/ARGANS, Aug-2011.
- [43] G. Zibordi and K. J. Voss, "Chapter 3.1 - In situ Optical Radiometry in the Visible and Near Infrared," in *Optical Radiometry for Ocean Climate Measurements*, vol. 47, C. J. D. and A. C. P. Giuseppe Zibordi, Ed. Academic Press, 2014, pp. 247–304.
- [44] K. G. Ruddick, V. De Cauwer, Y.-J. Park, and G. Moore, "Seaborne measurements of near infrared water-leaving reflectance: The similarity spectrum for turbid waters," *Limnol. Oceanogr.*, vol. 51, no. 2, pp. 1167–1179, Mar. 2006.
- [45] N. Fox and M. C. Greening, "A guide to comparisons – organisation, operation and analysis to establish measurement equivalence to underpin the Quality Assurance requirements of GEO, versio-4, QA4EO-QAEO-GEN-DQK-004," GEO, 2010.
- [46] J. L. Mueller *et al.*, "Above-Water Radiance and Remote Sensing Reflectance Measurement and Analysis Protocols. In Ocean Optics Protocols For Satellite Ocean Color Sensor Validation, Revision 2." NASA/TM-2000-209966, Aug-2000.
- [47] C. D. Mobley, "Estimation of the remote-sensing reflectance from above-surface measurements," *Appl. Opt.*, vol. 38, no. 36, pp. 7442–7455, Dec. 1999.
- [48] A. Morel and B. Gentili, "Diffuse reflectance of oceanic waters. II. Bidirectional aspects," *Appl. Opt.*, vol. 32, no. 33, pp. 6864–6879, Nov. 1993.
- [49] A. Morel, K. J. Voss, and B. Gentili, "Bidirectional reflectance of oceanic waters: A comparison of modeled and measured upward radiance fields," *J. Geophys. Res. Oceans*, vol. 100, no. C7, pp. 13143–13150, Jul. 1995.
- [50] A. Morel and B. Gentili, "Diffuse reflectance of oceanic waters. III. Implication of bidirectionality for the remote-sensing problem," *Appl. Opt.*, vol. 35, no. 24, pp. 4850–4862, Aug. 1996.
- [51] "Reference Model for MERIS Level 2 Processing Third MERIS reprocessing: Ocean Branch, PO TN MEL GS 0026 Issue 5." ESA/ARGANS, May-2013.
- [52] A. Morel, D. Antoine, and B. Gentili, "Bidirectional reflectance of oceanic waters: accounting for Raman emission and varying particle scattering phase function," *Appl. Opt.*, vol. 41, no. 30, pp. 6289–6306, Oct. 2002.
- [53] M. Gergely and G. Zibordi, "Assessment of AERONET-OC L WN uncertainties," *Metrologia*, vol. 51, no. 1, p. 40, 2014.
- [54] "IOCCG, International Network for Sensor Inter-comparison and Uncertainty Assessment for Ocean Color Radiometry (INSITU-OCR) White Paper, available from [http://www.ioccg.org/groups/INSITU-OCR\\_White-Paper.pdf](http://www.ioccg.org/groups/INSITU-OCR_White-Paper.pdf), 2012." [Online]. Available: [http://www.ioccg.org/groups/INSITU-OCR\\_White-Paper.pdf](http://www.ioccg.org/groups/INSITU-OCR_White-Paper.pdf). [Accessed: 07-Feb-2017].
- [55] "IMOS, A proposal for the creation of an "IMOS Radiometry Task Team (IRTT), 29 April 2016," 2016. [Online]. Available: [http://imos.org.au/fileadmin/user\\_upload/shared/IMOS%20General/documents/Task\\_Teams/IMOS-Radiometry-TaskTeam-Proposal-29April2016.pdf](http://imos.org.au/fileadmin/user_upload/shared/IMOS%20General/documents/Task_Teams/IMOS-Radiometry-TaskTeam-Proposal-29April2016.pdf). [Accessed: 10-Feb-2017].
- [56] J. Gröbner *et al.*, "Traveling reference spectroradiometer for routine quality assurance of spectral solar ultraviolet irradiance measurements. - PubMed - NCBI," *Appl. Opt.*, vol. 44, no. No25, pp. 5321–31, Sep. 2005.
- [57] G. Hülsen *et al.*, "Traceability of solar UV measurements using the Qasume reference spectroradiometer," *Appl. Opt.*, vol. 55, no. 26, pp. 7265–7275, Sep. 2016.
- [58] K. J. Voss, B. C. Johnson, and M. A. Yarbrough, "IOCCG, MOBY site and uncertainties," Esrin, Italy, 2013.
- [59] "PMOD/WRC, The World Calibration Center - Ultraviolet Section." [Online]. Available: [https://www.pmodwrc.ch/wcc\\_uv/wcc\\_uv.php?topic=wcc\\_uv\\_facility](https://www.pmodwrc.ch/wcc_uv/wcc_uv.php?topic=wcc_uv_facility). [Accessed: 10-Feb-2017].



- [60] D. Antoine *et al.*, “The ‘BOUSSOLE’ Buoy—A New Transparent-to-Swell Taut Mooring Dedicated to Marine Optics: Design, Tests, and Performance at Sea,” *J. Atmospheric Ocean. Technol.*, vol. 25, no. 6, pp. 968–989, Jun. 2008.
- [61] “FieldCAL. Spectral field calibration device for RAMSES radiometer.” [Online]. Available: [http://www.rshydro.co.uk/PDFs/Trios/fieldcal\\_en.pdf](http://www.rshydro.co.uk/PDFs/Trios/fieldcal_en.pdf). [Accessed: 10-Feb-2017].
- [62] “TriOS Ramses hyperspectral radiometers. User manual.” TriOS GmbH, 2004.



## Appendix A Sample device file of a TriOS RAMSES spectroradiometer

```
[Device]
Version          = 0
IDDevice         = SAM_81B0
IDDeviceType     = SAM
IDDeviceTypeSub1 = ARC
IDDeviceTypeSub2 = VIS
IDDeviceTypeSub3 =
RecordType       = 0
DateTime         = 2007-11-02 16:48:40
IDDeviceMaster   =
Comment          = ARC VIS

[Attributes]
DarkPixelStart = 237
DarkPixelStop  = 254
Firmware       = 2.04
IDDDataBack    = DLAB_2007-11-02_14-15-00_174_578
IDDDataCal     = DLAB_2007-11-02_16-48-12_664_300
IDDDataCalAQ   = DLAB_2007-11-02_16-48-15_835_301
IntegrationTime = 0
Reverse        = 0
SerialNo_MMS   = 036033
WavelengthRange = 310..1100
c0s            = 299.566
c1s            = 3.32347
c2s            = 0.000498784
c3s            = -1.96558e-06
c4s            = +0.000000000E+00
[END] of [Attributes]
[END] of [Device]
```





## Appendix B Factory proposed data processing method for TriOS RAMSES spectroradiometers

The following data processing example for a TriOS RAMSES hyperspectral radiometer is derived from the manufacturer's user manual [62].

Every radiometer has its own unique identification number (marked as "IDDevice" in the device file, see Appendix A). The identification number starts with letters "SAM" (Spectral Acquisition Module) or SAMIP (Inclination/Pressure), followed by four-digit hexadecimal code, e.g. SAM\_81Bo. Each module is equipped with a set of factory-provided device files, most important of which are:

- device file: SAM\_81Bo.ini
- background file: Back\_SAM\_81Bo.dat
- in-air calibration coefficients: Cal\_SAM\_81Bo.dat
- in-water calibration coefficients: CalAQ\_SAM\_81Bo.dat.

All of those are human-readable ASCII text files and could be modified, when necessary, by owner or a calibration laboratory. The files can be used, presumably in read-only mode, by the TriOS proprietary data acquisition and processing program "msda\_xe" or by any user-defined software tool. The files will be shortly described here in order to help understanding the following data processing example. Only the fields required for actual data processing will be listed.

### **SAM\_81Bo.ini**

IDDevice = SAM\_81B0  
Identification number, unique for each radiometer.

DateTime = 2007-11-02 16:48:40  
The file release time.

IDDataBack = DLAB\_2007-11-02\_14-15-00\_174\_578  
IDDataCal = DLAB\_2007-11-02\_16-48-12\_664\_300  
IDDataCalAQ = DLAB\_2007-11-02\_16-48-15\_835\_301

Identification of calibration data. The fields should equal to the fields named "IDData" in the corresponding background and calibration files.

DarkPixelStart = 237  
DarkPixelStop = 254  
Pixel numbers (in the range of 1..256) corresponding to the "dark pixels" used for bias compensation.

c0s = 299.566  
c1s = 3.32347  
c2s = 0.000498784  
c3s = -1.96558e-06  
c4s = +0.000000000E+00

Polynomial coefficients to convert the pixel number (1..256) into corresponding CWL.

### **Back\_SAM\_81Bo.dat**

IDData = DLAB\_2007-11-02\_14-15-00\_174\_578  
Unique data identification number

IDDevice = SAM\_81B0  
The radiometer the data belongs to.

DateTime = 2007-11-02 14:08:21  
Calibration timestamp

```
[DATA]
0 12 0 0
1 0.0213276433945366 0.0239517164074055 0
2 0.0211929064894141 0.0237542798616847 0
...
255 0.0218660824158588 0.0243825727941936 0
```

[END] of [DATA]

Background data for each pixel. First column contains pixel number (0..255), the second and third columns represent linear interpolation coefficients for each pixel, called *back1* and *back2*, respectively.

### **Cal\_SAM\_81Bo.dat, CalAQ\_SAM\_81Bo.dat**

IDData = DLAB\_2007-11-02\_14-15-00\_174\_578

Unique data identification number

IDDevice = SAM\_81B0

The radiometer the data belongs to.

DateTime = 2007-11-02 14:08:21

Calibration timestamp

IDDataBack = DLAB\_2007-11-02\_14-15-00\_174\_578

Corresponding background spectrum.

IntegrationTime = 64

Integration time during calibration, ms.

Unit2 = \$04 \$04 1/Intensity (m<sup>2</sup> nm Sr)/mW

Physical unit of the calibration coefficients.

```
[DATA]
0 5 0 0
1 +NAN 0 0
2 +NAN 0 0
3 +NAN 0 0
4 +NAN 0 0
5 0.453377173614255 0 0
...
255 +NAN 0 0
```

[END] of [DATA]

Calibration coefficients for each pixel in range of 0...255. First column contains pixel number, and the second column – calibration coefficient for the given pixel *cal*. The calibration coefficients have been normalized to 8192 ms integration time.

The user is encouraged to save the field (or calibration) data in plain text format to ease the following processing. Example of output file produced by the *msda\_xe* program will be described next.

### **SAM Control\_SAM\_81Bo\_Spectrum\_RAW\_11-49-46\_039.dat**

IDData = DB43\_2006-06-09\_11-49-44\_660\_034

Unique identification number of the measured spectrum.

IDDevice = SAM\_81B0

The radiometer the data belongs to.

DateTime = 2006-06-09 11:49:44

Measurement timestamp.

Comment =  
CommentSub1 =  
CommentSub2 =  
CommentSub3 =

User comments added during the data acquisition.

IDDataBack = DLAB\_2006-05-04\_09-36-37\_617\_548

IDDataCal = DLAB\_2006-05-04\_10-01-54\_871\_020

Identifiers of the background and calibration data relevant at the acquisition time.

IntegrationTime = 64

Integration time, in ms.

```
[DATA]
0 5 0 0
1 1509 0 0
2 1516 0 0
...
255 1452 0 0
[END] of [DATA]
```

Raw spectral data. First column contains pixel number  $n$  (0...255) and the second column – ADC counts for the given pixel, named  $So(n)$ . Data value for the  $n$ 'th pixel contains integration time, encoded in the lowest 4 bits. The integration time can be evaluated as follows:

$$it = 2^{1+(SO(0)AND0x0F)} \text{ ms.}$$

## Data processing

Pre-requirements for the data processing are

- raw spectrum  $So(n)$
- integration time (ms),  $it$
- background spectra  $back1(n)$ ,  $back2(n)$
- calibration spectrum  $cal(n)$ .

The following steps are necessary to convert the raw data into calibrated spectrum.

- 1) Calculate the wavelength scale, i.e. CWL for each pixel  $n$ :

$$\lambda(n) = c0s + c1s \cdot (n+1) + c2s \cdot (n+1)^2 + c3s \cdot (n+1)^3 + c4s \cdot (n+1)^4, n=(0...255).$$

- 2) Calculate the background spectrum:

$$back(n) = back1(n) + back2(n) \frac{it}{8192}.$$

- 3) Normalize the raw spectrum and subtract background:

$$S1(n) = \frac{SO(n)}{65535} - back(n).$$

- 4) Calculate average signal from the dark pixels:

$$SD = \frac{1}{DarkPixelStop - DarkPixelStart + 1} \sum_{n=DarkPixelStart}^{DarkPixelStop} S1(n).$$

- 5) Subtract dark signal and apply calibration coefficients:

$$L(n) = \frac{S1(n) - SD}{cal(n)} \cdot \frac{8192}{it}.$$

- 6) Switch to the wavelength scale:

$$L(\lambda) = L[\lambda(n)].$$



This final value (radiance in our case) should have physical unit as stated in the calibration file, i.e. reciprocal of *Unit2*.

The data processing steps are illustrated in Figure 24.

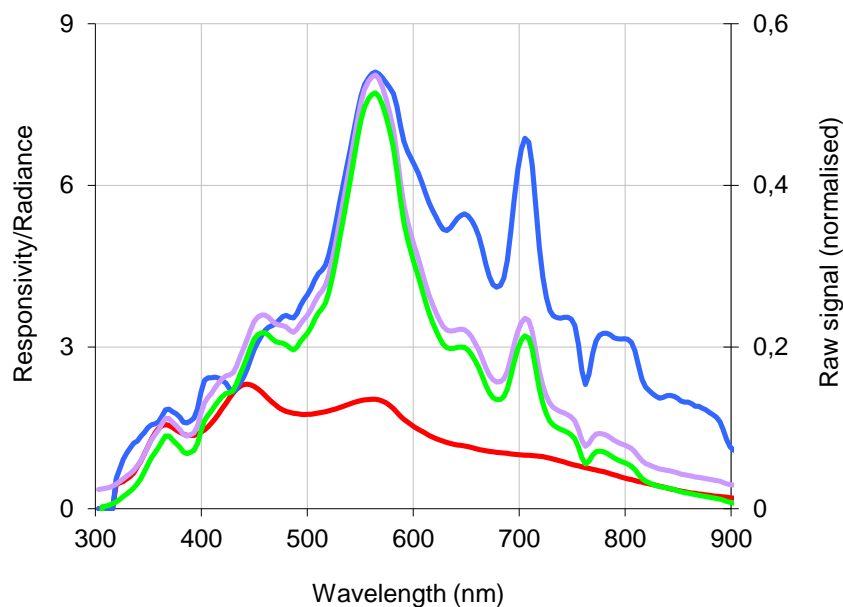


Figure 24: Processing raw TriOS data into calibrated values (SAM\_81Bo, upwelling water radiance).

Purple – raw ADC counts (normalised);  
green – raw data after background subtraction;  
red – spectral responsivity *cal* ( $\text{m}^2 \text{nm Sr mW}^{-1}$ );  
blue – spectral radiance ( $\text{mW m}^{-2} \text{nm}^{-1} \text{Sr}^{-1}$ ).

## Appendix C Indoor comparison

All participants are expected to send the equipment and related software to TO as follows:

- Radiometers, cables, power supplies etc., at least 2 weeks in advance to LCE-2. Controlling computers are not required, except in special cases.
- Controlling software, device and software manuals, calibration files etc., at least 4 weeks in advance to LCE-2. The software should be provided as electronic mail attachment or direct download link. Distribution of data by removable media (memory sticks, external drives, floppies etc.) is prohibited.

### C.1 Using the cleanroom

The indoor comparison exercise takes place in the optical laboratory of TO following the ISO 8 cleanroom standards and quality management system of TO. The general rules using the laboratories are covered by the following documents:

- Access to the laboratories (PL.4)
- Laboratory rules and regulations (PL.5)
- Safety in laboratories (PL.10).

Participants are expected to read these documents and confirm it with signature before entering the cleanroom area. The radiometers, measurement equipment and accessories will be transferred to the cleanroom in advance by the TO's dedicated personnel. The main rules to consider in the cleanroom are:

- Access only by a personal access card
- Wearing of special cleanroom suits and hats
- No drinks or food
- No personal belongings

In addition, the general rules for working with optical instruments apply.

### C.2 Measurement instructions

Measurement setup and calibration sources will be prepared and maintained by TO's dedicated personnel. During all steps, the intercomparison exercise will be monitored by TO's supervisor. The supervisor might divide the measurement into time intervals, called "station". The participant is expected to set up the radiometer under test and acquire measurement data as follows.

#### C.2.1 Irradiance sensors:

Refer to Figure 17.

1. connect all the necessary cables and power on the radiometer at least 30 minutes before the measurements
2. clean the input window of the sensor, if necessary;
3. install the temporary dual-beam alignment laser;
4. install radiometer under test using any of the supports available;
5. position the centre of the cosine collector along the laser beam
6. rotate and tilt the radiometer to be parallel to the optical axis
7. set up the distance between alignment jig and radiometer using a special tool
8. repeat steps 4)..6) until no further adjustments are needed.

After the final alignment is approved by the TO's supervisor, the data should be collected as follows:

1. the radiometer readings acquired in series of 30 readings;
2. at least three sets of series separated by no less than one minute interval;
3. the readings should be, whenever possible, taken at three different manually controlled integration times. The longest integration time should be chosen to align the raw signal maximum close (but not exceeding) the saturation level; the other two integration times approximately 2 and 4 times shorter;

4. each recorded value will be equipped with timestamp, integration time, station name provided by the supervisor, and any necessary metadata;
5. recording of the raw data (preferably in human-readable text files) is obligatory; storing of the derived irradiance values is up to the user.
6. Remove the instrument only after approved by the TO's supervisor.

### C.2.2 Radiance sensors:

Refer to Figure 18.

The user should align the radiometer (after cleaning the cosine collector, if necessary) along the optical axis crossing the centre of the sphere's output port as follows:

1. connect all the necessary cables and power on the radiometer at least 30 minutes before the measurements
2. the sensor's input window is aligned symmetrically in both the vertical and horizontal directions;
3. distance between the sensor and the sphere is chosen so that the diameter of the output port exceeds the one determined by sensor's FOV by at least factor of two;
4. after proper alignment, minor adjustments of the sensor in any direction should not change the raw output signal evidently.

After the final alignment is approved by the TO's supervisor, the data should be collected as follows:

1. the radiometer readings acquired in series of 30 readings;
2. at least three sets of series separated by no less than one minute interval;
3. the readings should be, whenever possible, taken at three different manually controlled integration times. The longest integration time should be chosen to align the raw signal maximum close (but not exceeding) the saturation level; the other two integration times approximately 2 and 4 times shorter;
4. each recorded value will be equipped with timestamp, integration time, station name provided by the supervisor, and any necessary metadata;
5. recording of the raw data (preferably in human-readable text files) is obligatory; storing of the derived irradiance values is up to the user.

Remove the instrument only after approved by the TO's supervisor.



## Appendix D Primary outdoor comparison

The primary outdoor comparison exercise takes place at lake Kääriku (Figure 5). The radiometers will be set up on the highest platform of the tower while the controlling computers, power supplies etc. will reside on the lower platforms. Mains power 230 VAC (up to 1.5 kW) will be available during the exercise.

The radiometers will be set up by TO's personnel in advance using the frames prepared previously. The input windows are cleaned, if necessary. Responsibility of the participants will be:

1. setting up computers, power supplies and any necessary devices on the lower platforms of the tower;
2. routing and attaching the instrument cables;
3. synchronizing internal clocks of computers and instruments to the UTC;
4. ensuring that all instruments are in operating condition and batteries fully charged;
5. preparing the controlling software for data acquisition with short notification time;
6. preparing logbook for instant measurement data.

The following terms apply to the data acquisition and are on the responsibility of the participants:

1. each recorded value will be equipped with timestamp, station name, integration time and any necessary metadata;
2. recording of the raw values (preferably in human readable text files) is obligatory; storing of the calculated results is up to the user.

The measurement plan is as follows. Radiometer positioning, start and stop of the data acquisition intervals are maintained by a exercise supervisor, determined by TO.

1. the irradiance sensors are installed in permanent positions during the exercise;
2. the radiance sensors are attached to the common frame, allowing simultaneous selection of azimuth and elevation angles;
3. checking, and if necessary, cleaning the input windows of the radiometers is the responsibility of TO's personnel;
4. the frame with radiance sensors will be operated by the supervisor;
5. sequence of pointing angles for the radiance sensors are selected, stated as "station";
6. start and stop times for each station are clearly announced;
7. duration of each station depends on weather conditions and instrument requirements, the approximate expected value is 30 seconds;
8. participants should collect instrument data in tight relationship to the station start and stop times;
9. related obligatory metadata, such as measurement geometry, environmental conditions etc. will be provided by supervisor.
10. participants are allowed to collect additional data relevant to the exercise, while giving highest priority to the primary radiometric quantities needed for the intercomparison.
11. participants should clearly announce about the possible technical problems and/or issues related to the data quality.
12. between the stations, participants are expected to perform initial check and backup of the previously collected data, check the battery levels etc.;
13. the end of the exercise will be announced by the supervisor;
14. Participants are allowed to deinstall the equipment.

## Appendix E Secondary outdoor comparison

The secondary outdoor comparison exercise takes place at lake Kääriku (Figure 5). The radiometers will be set up on the platforms of various height of the tower and pier. During the exercise, mains power 230 VAC (up to 1.5 kW) will be available.

The radiometers will be set up by participants, taking into account recommendations from the TO's personnel. Responsibility of the participants will be:

1. setting up the radiometers in the typical field measurement configuration;
2. cleaning the radiometers' input windows if necessary (DI water, isopropyl alcohol and lens cleaning wipes will be made available to participants);
3. setting up computers, power supplies and any necessary devices;
2. routing and attaching the instrument cables;
3. synchronizing internal clocks of computers and instruments to the UTC;
4. ensuring that all instruments are in operating condition and batteries fully charged;
5. preparing the controlling software for data acquisition with short notification time;
6. preparing logbook for instant measurement data.

The following terms apply to the data acquisition and are on the responsibility of the participants:

1. each recorded value will be equipped with timestamp, station name, integration time and any necessary metadata;
2. recording of the raw values (preferably in human readable text files) is obligatory; storing of the calculated results is up to the user.

The measurement plan is as follows. Suggested measurement geometry, start and stop of the data acquisition intervals are maintained by an exercise supervisor, determined by TO.

1. pointing of the sensors will be done by the participant;
2. start and stop times for each station are clearly announced;
3. duration of each station depends on weather conditions and instrument requirements, the approximate expected value is 30 seconds;
4. participants should collect instrument data in tight relationship to the station start and stop times;
5. participants are expected to log measurement geometry of their instruments and to not change it within a station;
6. related obligatory metadata, such as environmental conditions etc. will be provided by supervisor.
7. participants are allowed to collect additional data relevant to the exercise, while giving highest priority to the primary radiometric quantities needed for the intercomparison.
8. participants should clearly announce about the possible technical problems and/or issues related to the data quality.
9. between the stations, participants are expected to perform initial check and backup of the previously collected data, check the battery levels, clean the input windows if necessary etc.;
10. the end of the exercise will be announced by the supervisor;
11. Participants are allowed to deinstall the equipment.

## Appendix F      Data dissemination

Calibration data for the instruments will be maintained by the pilot (TO) and distributed to the participants within 4 weeks after LCE-2. Initial data screening and splitting between stations will be performed by the participants. The participants are expected to send the data to the pilot within 4 weeks after LCE-2. The data should meet the following criteria:

- Every dataset is associated with corresponding indoor or outdoor station name;
- Each recorded value is equipped with timestamp, integration time (or gain factor) and any necessary metadata;
- Data are in raw unprocessed values whenever possible, with associated dark readings.

Uncertainty budgets are compiled by TO and NPL. Results of the indoor and outdoor comparison exercises will be disseminated in TR-6 "Results from the First FRM4SOC Field Ocean Colour Radiometer Verification Round Robin Campaign".